THE INFLUENCE OF SOUND UPON LAMINAR BOUNDARY LAYER INSTABILITY

by

PAUL J. SHAPIRO

Report No. 83458-83560-1

September 1977

This research was carried out under the Fluid Mechanics Program of the National Science Foundation under Grant NSF Eng 75-17374 and the Fluid Dynamics Branch of the Office of Naval Research under Contract No. 00014-76-C-0396

ACOUSTICS AND VIBRATION LABORATORY

Massachusetts Institute of Technology
Cambridge, Massachusetts 02139

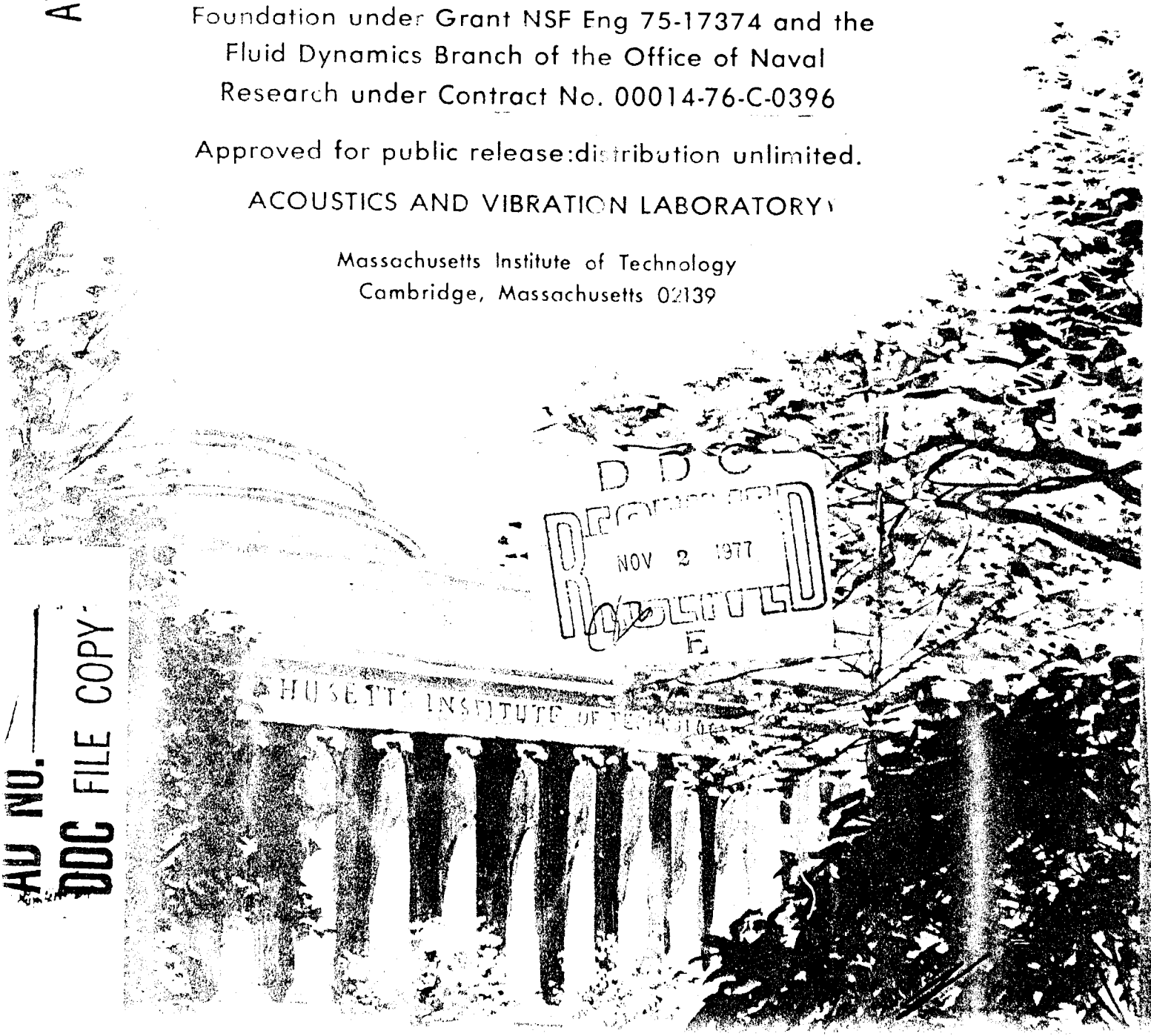

Unclassified

SECURITY CLASSIFICATION OF THIS PAGE (When Data Entered)

(14) NV-83458-83560-1

REPORT DOCUMENTATION PAGE

READ INSTRUCTIONS BEFORE COMPLETING FORM

1. REPORT NUMBER: Acoustics & Vibration Lab. 83458-83560 - 1

2. GOVT ACCESSION NO.

3. RECIPIENT'S CATALOG NUMBER

(9) Rept. for Oct 75-Sep 77,

4. TITLE (and Subtitle)

(6) The Influence of Sound Upon Laminar Boundary Layer Instability,

5. TYPE OF REPORT & PERIOD COVERED: October 1975 through September 1977

6. PERFORMING ORG. REPORT NUMBER

7. AUTHOR(s)

(10) Paul J. Shapiro

8. CONTRACT OR GRANT NUMBER(s)

(15) NSF-ENG-75-17374 & ONR N00014-76-C-0396

9. PERFORMING ORGANIZATION NAME AND ADDRESS

Massachusetts Institute of Technology
Cambridge, Massachusetts 02139

10. PROGRAM ELEMENT, PROJECT, TASK AREA & WORK UNIT NUMBERS

11. CONTROLLING OFFICE NAME AND ADDRESS

National Science Foundation, Washington, D.C. 20550 & Office of Naval Research, Arlington, Va 22217

(11) 12. REPORT DATE: September 1977

13. NUMBER OF PAGES: (12) 89p.

14. MONITORING AGENCY NAME & ADDRESS (if different from Controlling Office)

15. SECURITY CLASS. (of this report): Unclassified

15a. DECLASSIFICATION/DOWNGRADING SCHEDULE

16. DISTRIBUTION STATEMENT (of this Report)

Approved for public release; distribution unlimited

17. DISTRIBUTION STATEMENT (of the abstract entered in Block 20, if different from Report)

18. SUPPLEMENTARY NOTES

19. KEY WORDS (Continue on reverse side if necessary and identify by block number)

Laminar Boundary Layer
Transition
Sonic excitation
Tollmien-Schlichting waves

20. ABSTRACT (Continue on reverse side if necessary and identify by block number)

This paper presents the results of an experimental investigation into the effects of pure-tone acoustic excitation on Tollmien-Schlichting waves in a subsonic Blasius boundary layer. Longitudinal growth rates were measured for naturally-existing waves in a low-noise, low-turbulence wind tunnel, and for waves excited by an externally imposed sound field. The results were compared to numerical results from the standard Orr-Sommerfield equation.

DD FORM 1 JAN 73 1473 EDITION OF 1 NOV 65 IS OBSOLETE
S/N 0102-014-6601

Unclassified

SECURITY CLASSIFICATION OF THIS PAGE (When Data Entered)

405928

20

The excited Tollmien-Schlichting waves matched the theory well in most respects, and it was concluded that the acoustic excitation merely generated a larger initial wave amplitude, ahead of Branch I of the neutral stability curve. For excitation levels larger than the residual tunnel disturbances, this initial amplitude was constant and equal to the disturbance velocity of the sound wave. The naturally-existing waves showed growth rates smaller than the theory predicted. This leads to the conclusion that natural waves are not initially two-dimensional. Both cases showed spatial oscillations of the measured amplitude and phase, with a wavelength equal to the Tollmien-Schlichting wavelength. Since these oscillations were much more pronounced for the excited case, they may be related to the unknown coupling mechanism between the sound waves and the Tollmien-Schlichting waves.

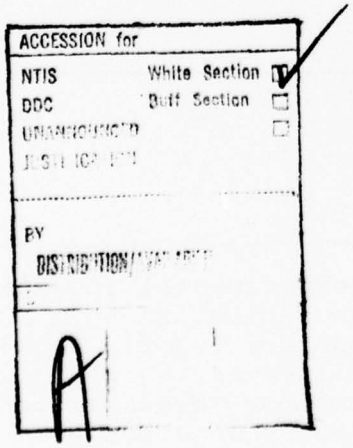

THE INFLUENCE OF SOUND UPON LAMINAR BOUNDARY LAYER INSTABILITY

by

Paul J. Shapiro

ABSTRACT

This paper presents the results of an experimental investigation into the effects of pure-tone acoustic excitation on Tollmien-Schlichting waves in a subsonic Blasius boundary layer. Longitudinal growth rates were measured for naturally-existing waves in a low-noise, low-turbulence wind tunnel, and for waves excited by an externally imposed sound field. The results were compared to numerical results from the standard Orr-Sommerfeld equation. The excited Tollmien-Schlichting waves matched the theory well in most respects, and it was concluded that the acoustic excitation merely generated a larger initial wave amplitude, ahead of Branch I of the neutral stability curve. For excitation levels larger than the residual tunnel disturbances, this initial amplitude was constant and equal to the disturbance velocity of the sound wave. The naturally-existing waves showed growth rates smaller than theory predicted. This leads to the conclusion that natural waves are not initially two-dimensional. Both cases showed spatial oscillations of the measured amplitude and phase, with a wavelength equal to the Tollmien-Schlichting wavelength. Since these oscillations were much more pronounced for the excited case, they may be related to the unknown coupling mechanism between the sound waves and the Tollmien-Schlichting waves.

ACKNOWLEDGEMENTS

I would like to thank my supervisor, Professor Patrick Leehey, for his general help and encouragement during the two-year duration of this project. Professor Steven Orszag's advice and theoretical calculations were of great assistance, as were Professor C. Forbes Dewey's recommendations and contributions during the writing. Others contributed their aid, particularly Mr. Todd Harland-White, Dr. Robert Van Houten, and Mr. Robert Powell. The help of Ms. Cheri Gibson and Ms. Elaine Govoni, both in organizing and preparing the manuscript, was gratefully appreciated.

The financial support of the Office of Naval Research and the National Science Foundation is thankfully acknowledged, as is the support from my parents, Mr. and Mrs. George Shapiro. Last, but certainly not least, the support of Ms Amy Berger was present throughout.

TABLE OF CONTENTS

LIST OF FIGURES

CHAPTER 1

INTRODUCTION

The modern investigation of the process of boundary layer transition from laminar to turbulent flow was begun by Schubauer and Skramstad (1948). Making use of an excellent, low-turbulence wind tunnel, they were able to demonstrate experimentally all of the important features of the Tollmien-Schlichting instability theory. They also made the first quantitative measurements of the effect of free-stream turbulence on the transition Reynolds number. Their measurements showed that the transition Reynolds number with no static pressure gradient reached a constant value of 2.8×10^6 for free-stream turbulence levels below $u'/U_\infty = .1\%$. They noted that at these very low turbulence levels, the measured turbulence appeared to be due primarily to acoustic disturbances, and suggested that this might be an important fact. They further reported that they could excite the Tollmien-Schlichting waves with sound, thereby reducing the transition Reynolds number.

Investigations subsequent to those of Schubauer and Skramstad focused on the nonlinear stages of boundary layer transition. More recently, however, Wells (1967) and Spangler and Wells (1968) have re-examined the effect of free-stream turbulence on transition Reynolds number.

Their tunnel, in addition to having low turbulence, was designed to have a low level of background acoustic noise. They reported a value of 5.2×10^6 for the transition Reynolds number at low turbulence levels and, presumably, at zero pressure gradient. They attributed the difference between their results and those of Schubauer and Skramstad to the fact that the acoustic levels in their tunnel represented only a small fraction, estimated at less than 20%, of the measured free-stream turbulence. Thus, they implied that an acoustic disturbance with a given RMS velocity level is somehow more destabilizing to the boundary layer than a free-strear turbulence field of the same velocity. They went on to show that different sound fields had different effects on transition (Figure 1). At the present time, the Spangler and Wells experiment is the only one to have reached a transition Reynolds number as high as 5×10^6.

The purpose of this investigation was not to repeat the Spangler and Wells measurements, but rather to look at the detailed effects of acoustic excitation on the first stage of transition, the Tollmien-Schlichting waves. It has been shown by Morkovin and Paranjape (1971), Sato (1960), Sato and Kuriki (1961), Brown (1935) and Miksad (1970) that sound fields can have a large adverse effect on the

stability of free jets, free shear layers, and wakes. Grosch and Salwen (1968) have developed a theory which predicts that incompressible plane Poiseuille flow can be either stabilized or destabilized by oscillating pressure gradients, as shown experimentally by Miller and Fejer (1964) and Obremski and Fejer (1967). Several investigators in addition to those previously mentioned have suggested that sound has a significant effect on the transition of a laminar boundary layer. See, for example, Pfenninger and Reed (1966), Vlasov and Ginevskii (1971), Knapp and Roach (1968), von W. Schilz (1965) and Boltz,Kenyon and Allen (1960). The only theoretical treatment of this problem was published by Mack (1975) for the case of supersonic flow.

The subsonic theoretical problem differs substantially from the supersonic case, in that it is no longer clear how to represent the acoustic excitation. The theoretical solution for incompressible Poiseuille flow was possible because the Navier-Stokes equations in this case are truly linear, resulting in an exact, analytical solution for the disturbed mean flow. The Blasius boundary layer is not a parallel mean flow, although most stability calculations treat it as such and give results which compare well to experiments and to more rigorous calculations. The boundary layer equation is not even valid at the extreme leading edge of a plate. Thus, at the present time, an experimental approach seemed more likely to succeed

in describing the effects of sound on laminar boundary layer instability than a theoretical one.

The objective of this study was to determine the effects of sound excitation on the linear disturbance growth stage of transition on a flat plate at zero pressure gradient in subsonic flow. These conditions were chosen since they are the most commonly and easily studied and best understood. The first question raised is whether the response to sound excitation is still of the same nature as the unexcited boundary layer transition process. Does the sound excite only Tollmien-Schlichting waves, or is some other mode of the boundary layer involved? The theory which predicts the Tollmien-Schlichting waves certainly permits other modes of response. Both discrete modes, one of which is the Tollmien-Schlichting wave, and continuous modes have been identified by Mack (1976) and Grosch (1977) although the Tollmien-Schlichting wave is the only unstable infinitesimal mode, and hence is the most likely one to be seen experimentally.

If the response is principally described by a Tollmien-Schlichting wave, what effect does the sound have? The possibilities include a simple change in the initial conditions and a change in the rate of growth of the waves. A change in the initial conditions could

manifest itself in at least two ways. There could be a straightforward increase in the initial disturbance velocity ahead of Branch I (see Figure 2), or there could be a more complete channeling of the disturbance energy into the Tollmien-Schlichting waves and larger apparent growth rates without any change in the Tollmien-Schlichting mechanism.

When the system is approximately linear, we would expect the response to a pure tone excitation to be primarily a Tollmien-Schlichting wave of the same frequency. Tollmien-Schlichting waves have a phase speed which is typically one-third the free stream velocity while the phase speed of acoustic waves is the speed of sound in air, 345 m/sec. For a fixed frequency, the wavelength is directly proportional to the phase speed. Thus, at a typical test condition of 35 m/sec, the acoustic wavelength is 30 times larger than the appropriate Tollmien-Schlichting wavelength. Given this very poor match, how does the acoustic excitation couple to the Tollmien-Schlichting waves?

CHAPTER 2

BOUNDARY LAYER TRANSITION

The general nature of the process of boundary layer transition is fairly well understood today, although there is still much work to be done before theoretical descriptions of transition on arbitrary bodies in various environments can be calculated accurately. We present here a description of the transition process at subsonic speeds on a smooth, flat plate in a low-turbulence, quiet, constant-temperature fluid with zero static-pressure gradient over the plate. The steps remain qualitatively similar even when most of these restrictions are relaxed.

Transition is a process which is conveniently described using a body-fixed coordinate system. The beginning of the plate has a purely laminar boundary layer, described as a Blasius boundary layer except in the immediate vicinity of the leading edge, where the Blasius solution is not valid. The stability of this flow can be investigated mathematically by assuming the flow to be a Blasius flow plus an infinitesimal harmonic disturbance wave of arbitrary frequency or wavenumber. The flow is unstable if there is any disturbance which will grow once it is excited. If the flow is stable to all

infinitesimal disturbances, it must also be proven to be stable to finite disturbances. The case of an infinitesimal disturbance is a linear problem, whereas a finite disturbance by definition results in a nonlinear problem.

The linear stability of Blasius flow was first computed by Tollmien (1931) and Schlichting (1933), although the equations were first discussed by Lord Rayleigh (1887). A detailed description is given in Schlichting (1968), but the basis will be presented here. We are examining the stability of two dimensional Blasius flow. Squire (1933) proved that the most amplified disturbances in this case are also two dimensional, so we can neglect the spanwise dimension. The plate lies in the $y = 0$ plane, with x representing the distance downstream from the leading edge, y being the distance normal to the surface of the plate, and U_∞ being the free stream velocity in the x direction. The perturbation wave has a wave number $k = 2\pi/\lambda$, where λ is the wavelength, and a circular frequency ω. In non-dimensional form, the perturbation is represented by the real part of a stream function,

$$\psi = \phi(y/\delta^*) \exp\left[i\left(\alpha \frac{x}{\delta^*} - \beta \frac{U_\infty{}^2 t}{\nu}\right)\right],$$

where $\alpha = k\delta^*$ is the complex, dimensionless wave number and $\beta = \omega\nu/U_\infty{}^2$ is the complex, dimensionless frequency,

with the Blasius boundary layer displacement thickness, $\delta^* = 1.72\sqrt{\nu x/U_\infty}$. Since $x/\delta^* = (U_\infty \delta^*/\nu)(1/1.72)^2 = 1/(1.72)^2 R_{\delta^*}$, we can use R_{δ^*}, the displacement thickness Reynolds number, as the non-dimensional x parameter.

These variables and parameters are then inserted into the dimensionless Navier-Stokes equations for the perturbation field, resulting, after some manipulation {see Schlichting (1968)}, the assumption of parallel mean flow, and linearization, in the Orr-Sommerfeld stability equation. The parallel flow assumption neglects the boundary layer growth in x.

$$\phi^{iv} - 2\alpha^2\phi'' + \alpha^4\phi = iR[(\alpha U-\beta)(\phi'' - \alpha^2\phi) - \alpha U''\phi]$$

This is a fourth order, ordinary differential equation for $\phi(y/\delta^*)$, with the parameters $U(y/\delta^*)/U_\infty$, the unperturbed boundary layer velocity profile at a given R_{δ^*}, α and β. The boundary conditions stipulate that the perturbation velocities must go to zero at the plate and as $y \to \infty$. This equation represents an eigenvalue problem.

There are two methods of proceeding. If α is chosen as real and given, the problem involves solving for the complex eigenvalue β which will permit ϕ to satisfy the boundary conditions and the equation. The real part of β represents the required frequency of the perturbation for

the given wave-number while the imaginary part, β_i, represents exponential growth or decay in time. For stability calculations we are interested only in the first mode, which is the least stable one. This is known as the temporal problem, since the result gives a temporal growth rate. The opposite problem, that of spatial growth, is the case studied experimentally. A real frequency, β_r, is assumed and the complex wavenumber $\alpha = \alpha_r + i\alpha_i$ is solved for, with α_i giving the exponential growth or decay, for a single value of R_{δ^*}. Most commonly, the temporal problem is the one for which solutions have been given, even though spatial characteristics are necessary for comparison with experiments. Gaster (1962) proved that for small amplification rates, which is the case in the boundary layer, the spatial growth is related to the temporal growth by

$$\alpha_i = - \left(\frac{1}{\frac{\partial \beta_r}{\partial \alpha_r}} \right) \beta_i$$

where $- \partial\beta_r/\partial\alpha_r$ is the group velocity of the wave. Briggs (1964) discusses a more general form of this relation.

The results of these various calculations can be presented in several ways. The neutral stability curve, along which there is neither growth nor decay, can be

plotted as shown in Figure 2, taken from Shen (1954). The easiest result to compare with an experimental measurement is a plot of the growth and decay of a single frequency as a function of R_{δ^*}, shown in Figure 3, from Ross, Barnes, Burns, and Ross (1970). The derivatives of these curves would be proportional to α_i, the spatial amplification rate. Figure 4, from the same source, shows some typical Tollmien-Schlichting wave velocity profiles across the boundary layer.

Returning to the flat plate transition process, the first stage of transition involves the growth of two-dimensional Tollmien-Schlichting waves. When these waves become sufficiently large, non-linear mechanisms cause the perturbation velocities to grow much more rapidly, leading to the formation of turbulent bursts. The intermittency, γ, of the boundary layer at any point is defined as the percentage of time the flow is turbulent. The most common definition of transition Reynolds number is the Reynolds number based on the x location where the maximum value of γ within the boundary layer is 50%. The importance of the Tollmien-Schlichting waves is due to the fact that the non-linear breakdown to turbulence occurs over a very short distance compared to the length of plate required for linear Tollmien-Schlichting growth, so that the transition

Reynolds number is primarily determined by the Tollmien-Schlichting amplification process. Further details of the non-linear aspects of transition may be found in Klebanoff and Tidstrom (1959), Klebanoff, Tidstrom and Sargent (1962), Hama and Nutant (1963), Kovasznay, Komoda and Vasudeva (1962), Landahl (1972), Tani (1969), and Reshotko (1976).

There are a large number of variables which can affect the transition process. The stability characteristics of the Tollmien-Schlichting waves are very sensitive to the exact shape of the velocity profile, U(y). "Fuller" velocity profiles, such as those associated with a favorable pressure gradient, are more stable, while any inflected profile, with $U''(y) = 0$, is rendered less stable. Obremski, Morkovin and Landahl (1969) give tables to permit stability calculations for a wide range of profiles. Velocity profiles are affected by an external pressure gradient, boundary layer suction or blowing, large, two-dimensional roughness, as shown by Klebanoff and Tidstrom (1972), polymer injection and heating or cooling of the plate relative to the fluid. Figure 5 shows the neutral stability curve and the value of the maximum growth rate for several pressure gradients.

Since stability theory only indicates the growth rate of a disturbance, the transition Reynolds number is strongly affected by the initial levels of the Tollmien-Schlichting waves as they enter Branch I of the neutral stability curve shown in Figure 2. Presumably this is how free-stream turbulence and small-scale surface roughness affect transition, although this is not certain. Mack (1977) presents an excellent discussion, and an empirical approach, of this problem.

Sound, as well as plate vibration, is a different sort of excitation because it is correlated over large distances, both longitudinally and spanwise, in general. It is therefore conceivable that the effects of sound on the boundary layer may be more complex than the effects of free-stream turbulence or roughness. Sound excitation probably increases initial Tollmien-Schlichting levels, but it may also change the stability characteristics.

Any discussion of the coupling of an excitation field to the boundary layer disturbances must include the question of the excitation spectrum. Previously mentioned experiments with sound excitation of the Blasius boundary layer have shown that excitation is only effective when it contains energy in the unstable Tollmien-Schlichting frequency range. Obremski and

Fejer (1967) have shown that for plane Poiseuille flow subjected to an oscillating pressure gradient there is a limiting frequency, for a given disturbance amplitude, above which there is no effect on transition. To be most meaningful, therefore, disturbances such as free-stream turbulence should be characterized by a power spectral density rather than by an overall RMS amplitude. Perhaps the more detailed description will eventually provide an explanation of the variations in transition Reynolds number as observed at different test facilities, and in the same facility at different test speeds (the unit Reynolds number effect). The unit Reynolds number is defined as the dimensional quantity U_∞/ν. Mack (1975) has had some success using this approach to treat supersonic boundary layer transition.

CHAPTER 3

EXPERIMENTAL FACILITY

WIND TUNNEL AND TEST APPARATUS

These experiments were performed in the M.I.T. Acoustics and Vibration Laboratory's wind tunnel (Figure 6). This was a low-turbulence, low-noise, open-circuit wind tunnel. The contraction ratio was 20:1, leading to a square test section 38 cm x 38 cm, 4 meters long. Tunnel speeds ranged from 11 m/sec to 50 m/sec. A special test section duct was built for this program. The inside walls were lined with an acoustically absorbing material, which presented a very smooth surface to the flow. These inner walls were false walls, not structural ones, and could be adjusted to control the pressure gradient. The measurements were made on a test plate which was mounted horizontally, and was supported on two longitudinal rails. The rails could be adjusted to control the angle of attack of the plate, and they also allowed the plate to be installed in different longitudinal locations within the test section.

The plate spanned the full 38 cm test section width, and was 170 cm long. It was fabricated as a composite sandwich, as shown in Figure 7. The top test surface was a piece of 0.25 inch thick aluminum tool and

jig plate. Beneath this surface was a 0.125 inch thick sheet of viscoelastic vibration-damping material (E-A-R C-1002, from E-A-R Corp., Westwood, Massachusetts), followed by a 0.125 inch thick aluminum sheet. The sandwich was bonded together with a two-part polyurethane adhesive, chosen for its high peel strength. This configuration was chosen to give very high levels of vibration damping. The calculated damping from Beranek (1971) depends on frequency and temperature, but ranged from 11% of critical damping at 2000 Hz and 25°C to 40% of critical at 500 Hz and 20°C. Critical damping is defined as the minimum amount of damping required to result in no oscillation when the system is given an initial displacement from its equilibrium. A thin splitter plate was mounted at the trailing edge to prevent coherent vortex shedding from creating plate vibrations.

The most difficult decision in the plate design was the shape of the leading edge. This had to be chosen to prevent flow separation, which would give rapid (almost instant) transition. A computer program for calculating inviscid flow near the leading edge of an airfoil was used to test several shapes.[1] From each of

[1]The computer program was kindly loaned by Professor Jerome Milgram, M.I.T., Department of Ocean Engineering. The calculations were performed by Dr. Michael Davis, a visiting professor from the University of New South Wales, Sydney, Australia.

the calculated pressure profiles, the most severe local adverse gradient was measured. This was used to calculate a local Pohlhausen parameter, which indicates the tendency towards boundary layer separation. Semi-elliptical shapes gave the best Pohlhausen values, with the largest axis ratio giving the best result. A compromise had to be made, however, because a larger axis ratio moved the region of adverse gradient farther back on the plate, where the boundary layer was less stable, since $R_{\delta*}$ was larger. We selected a 6:1 axis ratio, so the leading edge of the .5 inch thick composite plate was 1.5 inches long, giving an $R_{\delta*}$ at the end of the leading edge of 555 at 41 m/sec test speed.

The surface of the test plate, used for testing, had an RMS roughness of .6 μm, which is the same test surface roughness as the plate used by Schubauer and Skramstad (1948). We further polished and buffed the surface to a measured RMS roughness of .3 μm.

The primary measurements made in this experiment were the velocities near the plate. The measurements were made using a miniature hot-wire anemometer probe (Thermo-Systems, Inc. probe model 1261-T1.5) with a DISA 55D05 battery powered, constant temperature anemometer and 555D15 linearizer.

A traverse was built by Charles Stark Draper Labs to move the probe over the plate surface. The traverse was remotely controlled, driven by two small motors, since access to the test section while the tunnel was running was very inconvenient. The two degrees of freedom were longitudinally (along the plate) and vertically, (normal to the plate surface). The probe was always located on the spanwise centerline of the plate. The longitudinal positioning of the traverse was accurate to .1 inch, the vertical to .001 inch. The vertical zero location could be easily reset at each local position along the plate to account for any irregularities in the traverse mechanism. A static pressure tube could also be mounted in the traverse to permit measurement of the static pressure gradient.

The traverse mechanism was located on top of the test section, out of the flow. The probe was mounted in a thin, airfoil-shaped support which passed through a long slot in the test-section roof. The slot was sealed airtight along its length by two pieces of foam which were butted together at the slot (Figure 8).

One set of tests was performed using a vibrating ribbon similar to that employed by Schubauer-Skramstad (1948). A piece of 6.4 mm wide by 0.04 mm thick plastic ribbon was stretched

across the plate and extended through small slits in the sides of the test section. Tension was maintained by a weight hanging from one side of the ribbon, while the other side was excited at the desired frequency by a small shaker.

MODIFICATION OF THE WIND TUNNEL

Previous measurements of the free-stream turbulence level in the wind tunnel indicated an RMS disturbance velocity of about .15% of the free-stream velocity. This was felt to be too high a level to permit the study of boundary layer transition, since measurements such as Schubauer and Skramstad (1948) have shown that turbulence levels above .08 - .10% have an adverse effect on transition Reynolds number. We added additional damping screens and a settling section ahead of the contraction, intending to reach a level of .05% turbulence. Subsequent measurements showed turbulence levels ranging from .05% at 11 m/sec to .06% at 53 m/sec. These measurements were made with the wind tunnel in a closed-duct configuration. This configuration has continuous ducting from the tunnel entrance to the blower fan. For reasons to be discussed later, this program was carried out in an open-duct configuration (Fig. 6). The blockhouse surrounding the test section was sealed shut, so that several sections of ducting could be removed, leaving a two meter long test section, a 2 meter length of open jet, and a collector nozzle at the downstream blockhouse wall. This configuration showed a much higher free-stream turbulence of about .16%. Measurement of the frequency spectrum of the

free-stream turbulence velocity (Fig. 9) showed a broad peak at 2.5 Hz. This frequency is identical to the calculated Helmholtz resonance frequency of the blockhouse, with the test section and the muffler constituting the resonator necks. Therefore, measured turbulence values were highly dependent on the frequency range used in the measurement. At 41 m/sec with a low frequency cutoff of 10 Hz, the turbulence was .04%. With a 4 Hz cutoff, the level was .07%, and with a 1 Hz cutoff we had .16% turbulence. It was our belief that the low frequency energy did not affect the transition process, since it was well below the significant Tollmien-Schlichting frequency range. Spangler and Wells (1968) performed some experiments to measure the change due to a similar low frequency resonance in their tunnel, and found no change in the transition Reynolds number when the level was reduced 10 dB.

Appendix I has a further discussion of free-stream turbulence in the tunnel.

ACOUSTIC NATURE OF THE WIND TUNNEL

It was felt that the background tunnel noise levels were low enough for the tests planned. From a pragmatic point of view, the levels were already as low as could be achieved by any practical means. The tunnel structure was isolated from all external sources of vibration, including the fan and motor. The fan housing was covered with vibration damping material and had a foam lining. There was a muffler between the test section and the blower fan to reduce the sound propagating directly upstream. The open-jet configuration, with foam lining on the blockhouse walls, further reduced the noise entering the test section from the downstream end. The test section itself had a foam lining and the tunnel entrance faced a fiberglass barrier designed to prevent noise from being reflected or transmitted into the tunnel. The resulting test section noise spectra are shown in Figure 10.

Since we wished to study the effects of sound excitation, we also had to study the excited acoustic field in the test section. Early tests showed a very poor field, with large variations in sound pressure level throughout the test section, but subsequent modifications resulted in maximum overall variations of the order of 5 dB. A longitudinal profile is shown in Figure 11, and

details are given in Appendix II. The detailed testing described was necessary to ensure that our experimental results would not be related to the specific nature of the acoustic field generated, and would therefore not be test facility dependent.

TRANSVERSE CONTAMINATION OF THE LAMINAR FLOW FIELD

The first test of the experimental facility was the measurement of the transition Reynolds number as a function of test speed, using the hot wire. The result (Figure 12) showed acceptable values at higher test speeds, but below 50 m/sec the transition location seemed to be fixed near 67 cm. We then used a flow visualization paint to study the transition pattern over the entire span of the plate. The flow visualization technique, described by Maltby (1962), gave results shown in Figure 13.

The transition on the centerline was caused by the transverse spread of the turbulent wedges. The wedges beginning at the corners of the plate were expected, and were first described by Charters (1943). The inner set of wedges, beginning at points A and B of Figure 13, were the cause of the observed geometrical fixing of transition. Measurements showed that these wedges were caused by areas of increased turbulence intensity (Figure 14) in the wind tunnel. These areas were present even when the plate was not in the tunnel.

The cause of these peaks was unknown, but the solution was to avoid the problem. The plate was lowered 6.3 cm below the test section centerline where there were not any abnormal disturbances. Flow visualizations then showed that transition occurred naturally, unaffected by any transverse contamination, at all test speeds above about 35 m/sec.

There was still a unit Reynolds number effect, meaning that the transition Reynolds number was a function of test speed (Figure 15), but it was not due to transverse contamination.

EXPERIMENTAL CONDITIONS

The experiments were conducted with essentially zero longitudinal static pressure gradient (Figure 16). Free-stream turbulence spectra at 29 m/sec and 41 m/sec mean flow speed are shown in Figure 9. The flat spectral levels seen at the higher frequencies are due to electrical noise in the anemometer, which made it impossible to accurately measure these levels. The background acoustic levels are shown in Figure 10, which is calibrated both in sound pressure level and in the equivalent velocity. The acoustic plane wave relationship, $p = \rho c u$, was used to relate the measured sound pressure, p, to the acoustic velocity, u, using the density of air, ρ, and the acoustic phase speed, c, as in Morse and Ingard (1968).

The test plate vibration levels were measured with the tunnel running at test speed, with and without the exciting sound field present. The vibratory velocity of the plate in the quiet tunnel was less than .005 mm/sec at all test speeds and frequencies, while the velocity in the presence of a sound pressure level of 95 dB was less than .015 mm/sec. The disturbance velocity of a 95 dB SPL acoustic wave, for comparison, is 3 mm/sec. Thus, the vibration levels of the test plate were believed to be sufficiently low for this experiment.

INSTRUMENTATION

Since this was the first attempt made to measure naturally occurring Tollmien-Schlichting waves, we had to be able to extract the small portion of the hot-wire anemometer signal in which we were interested. This involved measuring velocities as small as 0.1 mm/sec in a 40 m/sec mean flow with an RMS turbulence velocity of 70 mm/sec. The problem was further compounded by the fact that the hot-wire probes used had a strong vibration resonance around 750 Hz, which was in the frequency range of our data. Figure 17 shows a frequency spectrum of the hot-wire signal at one measurement point in the boundary layer. Data could be read from spectra such as this, but it was very slow, accuracy was at best $\pm$ 1 dB, and signal to noise ratio was not very large.

Therefore, we used a narrow band filter to take the data. The instrument chain is shown in Figure 18. The B & K frequency analyzer had an extremely large dynamic range, so it was used to precondition the signal before going into the 5 Hz Spectral Dynamics filter. The overall system, excluding the anemometer and linearizer, had a signal to noise ratio of at least 20 dB for the smallest signals analyzed.

The weakest points in the instrumentation were the anemometer and linearizer. As mentioned earlier, they were

unable to measure the free-stream turbulence levels at the higher frequencies, due to a background noise level of approximately $3\mu v/\sqrt{Hz}$. A Thermo-Systems, Inc. Model 1050 anemometer was tried, but its noise level was also too high to make the desired measurements.

Tests were made to ensure that the previously mentioned vibration resonance of the hot-wire probe did not have any effect on the measured data. Spectra, such as that shown in Figure 17, were taken with several probes having different resonance frequencies. All of the spectra taken at the same location were identical, except for the location of the resonance spike.

CHAPTER 4

EXPERIMENTS

The basic data desired was the Tollmien-Schlichting amplitude spatial growth curves, such as those shown in Figure 3. These were measured for the natural Blasius boundary layer, with the lowest disturbance level attainable, and for the Blasius boundary layer excited by sound. This involved measuring the RMS disturbance velocities as a function of x. A comparison of the results for the two different cases would indicate whether or not there was a change in the growth rates.

The procedure for taking data had to insure that measurements were always made at the y-value where the Tollmien-Schlichting wave amplitude was a maximum (see Figure 4). We took measurements at several y-values centered around the one where the maximum occurred, to be certain that we had indeed measured the maximum amplitude at that x-position. This test was not made for every data point, but was repeated often enough to ensure that no errors occurred.

For each data run, measurements started near the beginning of the plate. Data was taken at each probe position for the natural case and the excited case in immediate succession. This allowed us to compare the two results without the possibility of an artifact due to gradual changes

in the hot-wire sensitivity. Such a change could occur, for instance, due to ambient temperature changes during the course of a six hour data run. The probe was then moved to the next x-position, and the measurements were repeated. Measurements were taken at successive positions until a value of x was reached where the Tollmien-Schlichting wave had grown and then decayed to a constant background level. If turbulent bursts began to form before this point was reached, the measurements were stopped at the onset of bursting, preventing transverse contamination of the data. An intermittency of $\gamma = .0002$ was sufficient for the time-averaged RMS velocity of the bursts to be greater than the Tollmien-Schlichting amplitude, making it impossible to measure the Tollmien-Schlichting amplitude.

The measurements described above gave Tollmien-Schlichting growth curves ($\ell n\ A/A_o$ vs. $R_{\delta *}$). We decided that the growth rates, $\alpha_i \delta^*$, would be the most useful final result. To get the values of α_i, we had to differentiate the growth curves. This was done by drawing a smooth line through the experimental data (hand fairing), and taking derivatives by picking three points at a time from the faired curve. The three points were used to describe a least-squares-fit straight line, whose slope was taken as the value of α_i at the center point of the three. Since α_i is the derivative of an experimental result, we would expect

to see larger variations in α_i than we would see in the growth curves themselves. For this reason, some previous investigators have presented growth curves rather than growth rates.

In addition to this primary data, which will be discussed later, several measurements of the Tollmien-Schlichting wave properties were made for comparison to the theory. Velocity spectra, such as that shown in Figure 17, were taken at a series of positions along the plate. From each of these, the frequency of the largest Tollmien-Schlichting wave was selected (1540 Hz in Figure 17), and plotted versus $R_{\delta *}$. These points should fall just inside Branch II of the neutral stability curve, since they represent the frequency of the most amplified disturbance at that point on the plate. Figure 19 shows that they do indeed match previous results very closely.

The Tollmien-Schlichting amplitude as a function of y was measured at several x-locations. Some of the results are shown in Figure 20, along with the theoretical curves, and again the agreement is quite reasonable. The discrepancies seen for the profiles at $R_{\delta *} = 760$ and 930 may be due to several factors. The constant amplitudes for $y/\delta > .8$ are due to the acoustic disturbances in the excited case, and to free-stream turbulence or anemometer noise in the natural case. The shift relative to the theory in the location of

the maximum amplitude may be due in part to the pressure gradient which existed so near the plate leading edge (5-8 cm). The shift may also be due to a slight error in the vertical positioning of the probe, since δ was only 1 mm for $R_{\delta^*} = 760$. The good match of the location of the peaks for the excited and unexcited cases is due to the fact that both sets of data were measured during the same traverse. This good match further precludes the possibility that the peak was due to the excitation field, assuring us that we were measuring Tollmien-Schlichting waves.

Measurements of the Tollmien-Schlichting wavelength were also made. This was only feasible for the excited case, in which the excitation signal could be used as a reference for phase measurements. The distance required for a 360° phase increase was one wavelength. All results were within 2% of the theoretical values.

While these measurements were not intended as tests of the Tollmien-Schlichting theory, the agreement was certainly good, and showed conclusively that we were measuring Tollmien-Schlichting waves.

CHAPTER 5

DATA EVALUATION AND CONCLUSIONS

The two different test conditions discussed will be the tests performed while the boundary layer was subjected to a sound field generated by a loudspeaker at the front of the wind tunnel (referred to as the excited case), and the tests made with the minimum possible disturbances in the wind tunnel environment (the unexcited, or natural, case). It was impossible, of course, to create an experimental situation that was truly unexcited, since there were always residual disturbances in the wind tunnel. The free-stream turbulence and acoustic background spectra were discussed earlier, (p. 31), and are shown in Figures 9 and 10.

All theoretical calculations presented for comparison to the data were performed by Professor S. A. Orszag, Department of Mathematics, Massachusetts Institute of Technology, using his numerical computer program described in Report Number NASA CR 2910 , June, 1977.

One important conclusion reached was that it was possible to measure naturally-occurring Tollmien-Schlichting waves with a good degree of repeatability. Figure 24, to be discussed later, gives an indication of the variation observed. This implies that at a given test speed there was a constant level of background disturbances existing in

this wind tunnel. Presumably, other wind tunnels have different background disturbance levels, and it is these background levels which determine the flat plate transition Reynolds number in each tunnel. The similarity of the results measured in most tunnels is probably due to the similarity of the background disturbance levels existing in most wind tunnels used for transition research. Further quantitative conclusions cannot be drawn because disturbance spectra have rarely been published in detail.

A second conclusion was that for both the excited and unexcited cases, there was an approximately constant disturbance amplitude ahead of Branch I of the neutral stability curve (Figure 2). This constant level will be defined as the initial Tollmien-Schlichting amplitude. Figure 21 shows some faired growth curve plots to demonstrate this. Figure 20 shows some amplitude distributions normal to the plate surface taken ahead of Branch I (R_{δ^*} less than 950), to show that the disturbance velocities actually were Tollmien-Schlichting waves. Tollmien-Schlichting waves existed even in this region of the plate where they were stable, excited either acoustically or by residual disturbances. The amplitude remained constant simply because the excitation remained constant as the waves progressed down the plate. If the excitation had been spatially localized, like a vibrating ribbon, the Tollmien-Schlichting amplitudes would

have decayed away from the source, until Branch I was reached, as shown by Schubauer and Skramstad (1948). In the excited case, the initial Tollmien-Schlichting amplitude corresponded very well to the velocity created by the acoustic excitation, once the exciting sound was loud enough to exceed the residual exciting disturbances. Figure 22 presents data which demonstrates that the initial Tollmien-Schlichting amplitude and the exciting acoustic velocity were proportional to one another, with a proportionality factor (or "coupling factor") equal to one, regardless of test speed or frequency. We have not, however, succeeded in identifying the coupling mechanism involved.

The next region to be examined is the Tollmien-Schlichting growth region, between Branch I and Branch II of the neutral stability curve. One can present either the growth curves ($\ln \frac{A}{A_o}$ vs. R_{δ^*}, Figure 21) or growth rate curves ($\alpha_i \delta^*$ vs. R_{δ^*}, Figure 23). Examination of either shows that there was significantly more growth in the excited case than in the unexcited. This difference was strongest over the first half of the growth region. Before the Tollmien-Schlichting waves reached Branch II, where the amplitudes began to decay, the growth rates for the two cases became equal. The decay rates, beyond Branch II, remained equal as far downstream as measurements could be made.

As the exciting sound pressure level was increased, the entire growth curve just shifted position (on a logarithmic scale) while the growth rates remained exactly the same. When measurements were made during the same data run with sound levels differing by 10.0 dB, all data points shifted 10.0 dB, within the 0.1 dB resolution of the measuring instrumentation. Thus, the excited growth rates reached a constant value once the sound was loud enough to overcome the residual disturbances. The question of which case, if either, matched the theory will be postponed, since there is another issue to be discussed first.

Data taken at different tunnel speeds should be identical when presented in the appropriate non-dimensional form. For growth rates, the correct variables are $\alpha_i \delta^*$ and R_{δ^*}. Systematic variations in the data represent the so-called "unit Reynolds number effect". The unit Reynolds number is the dimensional quantity, Reynolds number/unit length, $\frac{U_\infty}{\nu}$. Figure 24 shows data taken at two tunnel speeds. It is immediately apparent that the results are not identical, even within the limits of experimental repeatability.

Figure 25 shows a comparison of the static pressure distribution for the two test speeds, plotted as a function of R_{δ^*}. The region of adverse pressure gradient near the beginning of the plate occurred at different R_{δ^*} for the

two speeds, although, as expected, it was at the same x-position (Figure 16). The magnitude of the adverse gradient was worse at 41 m/sec (Falkner-Skan $\beta = -.07$) than at 29 m/sec ($\beta = -.03$). These values are only approximate, but the differences in magnitude and location of the adverse gradient agree qualitatively with the observed unit Reynolds number effect. Growth began earlier at 29 m/sec than at 41 m/sec because the adverse gradient began at a slightly lower $R_{\delta*}$. However, the maximum growth rates at 41 m/sec were larger because there was a stronger adverse pressure gradient, which aso persisted to a higher $R_{\delta*}$.

The problems created by the pressure gradient make it more difficult to decide whether the excited case showed larger than theoretical growth, or the natural case showed less than theoretical growth. At the beginning of the plate, the effect of the pressure gradient was to increase the measured growth rates above the values which would have been observed in a true zero pressure gradient. The unit Reynolds number effect should have disappeared at an $R_{\delta*}$ of about 1500, as seen from Figure 25. Figure 24 shows that the results did converge at this $R_{\delta*}$.

Figures 26 and 27 summarize the data by presenting the average of the results obtained in several runs at each of the two test speeds. Figure 27 shows three curves -- the theory for zero pressure gradient, the excited results, and

the natural case. Figure 26 has one additional curve, presenting data obtained in several runs using a vibrating ribbon similar to that employed by Schubauer-Skramstad (1948). Unfortunately, the ribbon would not sustain enough tension to raise its resonance frequency to the test frequency, so it was not a very good pure-tone exciter.

An attempt was made to take data with the ribbon positioned before Branch I, but the ribbon was too much of an obstruction in the thin boundary layer ($\delta^* = 0.42$ mm), and caused transition to occur immediately. Thus, only limited data of questionable reliability was obtained. It does, however, seem to agree somewhat more closely with the excited data than the unexcited data (Figure 26).

Based on the sum total of the above evidence and discussion, we conclude that the excited growth rates match the theoretical predictions of the Orr-Sommerfeld equation. We have previously seen that the phase velocity and normal mode shapes for the excited case also match the theory. Since the complex eigenvalue and the eigenmode measured agree with the Tollmien-Schlichting theory, the obvious conclusion is that acoustic excitation generates Tollmien-Schlichting waves of the same frequency as the excitation.

It remains to explain why the natural case shows less growth than the theory would predict. The theory applies to a two-dimensional Tollmien-Schlichting wave propagating

in the free-stream direction. It appears that naturally excited Tollmien-Schlichting waves are not two-dimensional, but are made up of waves having varying propagation directions. Thus, some portions of the disturbance velocity would grow more slowly than predicted, since until the point of maximum growth rate is reached, the two-dimensional Tollmien-Schlichting waves are the most unstable. Therefore, the initial growth rates of natural disturbances, averaged over all propagation directions, will be less than the theoretical and excited growth rates, both of which represent plane disturbances propagating in the free-stream direction. The most unstable Tollmien-Schlichting waves should eventually dominate the observed disturbances, in both the natural and excited cases. Therefore, the growth rates for the two cases should become identical for large enough R_{δ^*}, as shown in Figures 26 and 27. Very recently, Mack (1977) used a similar concept to develop an empirical method of predicting transition Reynolds numbers.

Before continuing, another possible interpretation of the data should be mentioned. It is quite possible that the different results obtained for the natural case at the two test speeds could be due to different disturbance environments. Figure 10 shows that the background sound levels increased by approximately 10 dB (a factor of 3.2)

when the test speed increased from 29 m/sec to 41 m/sec (a factor of 1.4). This change in environment may well contribute to the observed unit Reynolds number effect, and does not contradict our previous conclusions. There is, however, a contradictory hypothesis for the difference seen in the excited case. For $\beta_r = 56 \times 10^{-6}$, the ratio of the acoustic wavelength to the Tollmien-Schlichting wavelength at 41 m/sec is 25, while at 29 m/sec and the same β_r, the ratio is 36. Attempts to investigate the significance of this scale parameter by taking data at a wider range of tunnel speeds failed. At lower speeds we were limited by transverse contamination and low signal levels, while higher speeds necessitated working on the curved portion of the plate leading edge, with strong pressure gradients and extremely thin boundary layers. While the hypothesis of scale effects cannot be completely eliminated by the present experiments, Figure 22 shows that the measured coupling factor between the excitation and the Tollmien-Schlichting response is independent of this scale parameter. The previous conclusion, attributing the variation to a unit Reynolds number effect, seems much more logical.

The last item to be discussed involves a persistent peculiarity seen in the data. The growth curves shown in Figure 21 were identified as smoothed curves. The actual

data is shown in Figure 28. The peculiarity observed is that the measured amplitudes show spatial oscillations. While these oscillations were much larger for the excited data than the unexcited data, they were clearly present in all data. Oscillations of the same wavelength were observed when the excited Tollmien-Schlichting phase was measured as a function of x (Figure 29). Before Branch I was reached, the phase did not grow at all, it merely oscillated at the same wavelength. After Branch I, the phase grew regularly, as it should for a travelling wave, but when the steady, linear growth was subtracted from the data, the reduced phase showed the same oscillations.

These oscillations were purely spatial, since a 30 second averaging time was used for all measurements. The most noticeable property of the oscillations was that the wavelength always matched the Tollmien-Schlichting wavelength for that test condition. The first thought was that these oscillations were due to some sort of standing wave effect, but this seems unlikely since a standing wave has an observed wavelength equal to one-half the wavelength of the travelling wave. In addition, a standing Tollmien-Schlichting wave would imply that there were upstream-travelling waves, not a very likely possibility. No other measurements provided an explanation for these observed oscillations, which have

not been reported in the previous literature. They appear to be connected with the sound excitation, because the oscillation amplitude increases when the sound level increases. Furthermore, their presence has never been noted when a vibrating ribbon was used as the excitation source. Perhaps the oscillations are related to the coupling mechanism between the sound waves and the Tollmien-Schlichting waves. This is certainly one area which deserves further investigation.

REFERENCES

1. Beranek, L. L., Noise and Vibration Control. New York: McGraw-Hill Book Company, (1971).

2. Boltz, F. W., Kenyon, G. C., and Allen, C. Q., "The Boundary Layer Transition Characteristics of Two Bodies of Revolution, a Flat Plate, and an Unswept Wing in a Low-Turbulence Wind Tunnel", NASA TN D-309, (1960).

3. Briggs, R. J., Electron Stream Interaction with Plasmas, Research Monograph No. 29, MIT Press (1964).

4. Brown, G. B., "On Vortex Motion in Gaseous Jets and the Origin of Their Sensitivity to Sound", Proceedings of the Physical Society, 47, p. 703 (1935).

5. Charters, A. C., "Transition Between Laminar and Turbulent Flow by Transverse Contamination," NACA TN 891 (1943).

6. Gaster, M., "A Note on a Relation Between Temporally Increasing and Spatially Increasing Disturbances in Hydrodynamic Stability," J. of Fluid Mechanics, 14, p. 222 (1962).

7. Grosch, C. E., and Salwen, H., "The Stability of Steady and Time-Dependent Plane Poiseuille Flow," J. of Fluid Mechanics, 34, p. 177 (1968).

8. Grosch, C. E., "The Continuous Spectrum of the Orr-Sommerfeld Equation," Manuscript in Preparation.

9. Hama, F. R. and Nutant, J., "Detailed Flow-Field Observation in the Transition Process in a Thick Boundary Layer", Proc. of the 1963 Heat Transfer and Fluid Mechanics Institute, p. 77 (1963).

10. Klebanoff, P. S. and Tidstrom, K. D., "Evolution of Amplified Waves Leading to Transition in a Boundary Layer with Zero Pressure Gradient," NASA TN D-195, (1959).

11. Klebanoff, P. S., Tidstrom, K. D., and Sargent, L. M., "The Three-Dimensional Nature of Boundary-Layer Instability", J. of Fluid Mechanics, 12, p. 1 (1962).

12. Klebanoff, P. S., and Tidstrom, K. D., "Mechanism by which a Two-Dimensional Roughness Element Induces Boundary-Layer Transition", Physics of Fluids, 15, p. 1173 (1972).

13. Knapp, C. F., and Roache, P. J., "A Combined Visual and Hot-Wire Anemometer Investigation of Boundary-Layer Transition", AIAA Journal, 6, p. 29 (1968).

14. Kovasznay, L. S. G., Komoda, H. S., and Vasudeva, B., "Detailed FLow Field in Transition", Proc. of the Heat Transfer and Fluid Mechanics Institute, p. 1, (1962).

15. Landahl, M. T., "Wave Mechanics of Breakdown, Inst. of Fluid Mechanics, 56, p. 775, (1962).

16. Mack, L. M., "Linear Stability Theory and the Problem of Supersonic Boundary-Layer Transition", AIAA Journal, 13, p. 278 (1975).

17. Mack, L. M., "A Numerical Study of the Temporal Eigenvalue Spectrum of the Blasius Boundary Layer", J. of Fluid Mechanics, 73, p. 497 (1976).

18. Mack, L. M., "Transition and Laminar Instability", JPL Publication 77-15, to be published in Application and Fundamentals of Turbulence. (1977).

19. Maltby, R. L., "Flow Visualization in Wind Tunnels Using Indicators," NATO AGARDorgraph No. 70 (1962).

20. Miksad, R. W., "Experiments on Free Shear Layer Transition, Sc.D. Thesis, M.I.T., Department of Meteorology. (1970)

21. Miller, J. A. and Fejer, A. A., "Transition Phenomena in Oscillating Boundary-Layer Flows", J. of Fluid Mechanics, 18, p. 438 (1964).

22. Morkovin, M. V. and Paranjape, S. V., "On Acoustic Excitation of Shear Layers", Z. Flugwiss, 19, p. 328 (1971).

23. Morse, P. M. and Ingard, K. U., Theoretical Acoustics. New York: McGraw-Hill Book Company (1968).

24. Obremski, H. J. and Fejer, A. A., "Transition in Oscillating Boundary Layer Flows", J. of Fluid Mechanics, 29, p. 93 (1967).

25. Obremski, H. J, Morkovin, M. V., and Landahl, M., "A Portfolio of Stability Characteristics of Incompressible Boundary Layers", NATO AGARDograph 134, (1969).

26. Pfenninger, W., and Reed, V. D., "Laminar Flow Research and Experiments", Aeronautics and Astronautics, AIAA, p. 44 (1966).

27. Rayleigh, "On the Stability of Certain Fluid Motions", Proc. of the London Math Society, 19, p. 67 (1887).

28. Reshotko, E., "Boundary-Layer Stability and Transition", Annual Review of Fluid Mechanics, 8, p. 311, (1976).

29. Ross, J. A., Barnes, F. H., Burns, J. G., and Ross, M. A. S., "The Flat Plate Boundary Layer", J. of Fluid Mechanics, 43, p. 819 (1970).

30. Sato, H., "Transition of a Two-Dimensional Jet", J. of Fluid Mechanics, 7, p. 53 (1960).

31. Sato, H. and Kuriki, K., "The Mechanism of Transition in the Wake of a Flat Plate Placed Parallel to a Uniform Stream", J. of Fluid Mechanics, 11, p. 321, (1961).

32. Schlichting, H., "Zur Entstehung der Turbulenz bei der Plattenstromung", Nachr. Ges. Wiss. Gottingen, Math. Phys. Klasse, P. 181 (1933).

33. Schlichting, H. , Boundary Layer Theory. Sixth Edition. New York: McGraw-Hill Company (1968).

34. Schubauer, G. B. and Skramstad, H. K., "Laminar Boundary-Layer Oscillations and Transition on a Flat Plate", NACA Report 909, (1948).

35. Shen, S. F., "Calculated Amplified Oscillations in the Plane Poiseuille and Blasius Flows", J. of the Aeronautical Sciences, 21, p. 62 (1954).

36. Spangler, J. G. and Wells, C. S., "Effects of Freestream Disturbances on Boundary Layer Transition", AIAA Journal, 6, p. 503 (1968)

37. Squire, H. B., "On the Stability of Three-Dimensional Disturbances of Viscous Flow Between Parallel Walls", Proceedings of the Royal Society, A142, p. 621 (1933).

38. Tani, I., "Boundary Layer Transition," Annual Reviews of Fluid Mechanics, 1, p. 169 (1969).

39. Tollmien, W., "The Production of Turbulence", NACA TM 609 (1931).

40. Vlasov, Y. V. and Ginevskii, A. S., "Effect of Acoustic Disturbances on the Transition of Laminar Boundary Layer to Turbulent", Translation by NTIS, AD-A007446, 1975 (1971).

41. von W. Schilz, "Experimentelle Untersuchungen Zur Akustischen Beeinflussung Der Stromungsgrenzschicht in Luft", Acustica, 16, No. 4 (1965).

42. Wells, C. S., "Effect of Freestream Turbulence on Boundary Layer Transition, AIAA Journal, 5, p. 172, (1967).

APPENDIX I

FREE-STREAM TURBULENCE

At a later stage of the investigation, portions of the entrance section of the tunnel were sequentially removed in an attempt to increase the free-stream turbulence level. With just the soda-straw honeycomb, one damping screen, and the .6 meter long settling section ahead of the contraction, the turbulence levels were unchanged. This measurement was supported by the fact that the transition Reynolds number was also unaffected by the removal of the eight screens and duct sections.

These results deserve some comment, since it is generally felt that a large number of damping screens is necessary to achieve low turbulence levels. This wind tunnel had a 20:1 contraction ratio, which was larger than most. This helped reduce relative turbulence levels by increasing the mean flow speed by a factor of twenty while leaving the overall turbulence velocities essentially unchanged. Another feature of this tunnel which might have been relevant was the open circuit design. This may result in much lower levels of turbulence entering the tunnel than a more common closed circuit tunnel, which continuously recirculates any eddies generated.

In further attempts to increase turbulence, the honeycomb section was removed. The honeycomb was composed of soda straws, 0.25 inch in diameter and 12 inches long, giving a very large length to diameter ratio of 48. Removal of this section led to a pronounced increase in free-stream turbulence. With four screens on the front of the tunnel, at 41 m/sec, with a 10 Hz high pass filter, the level went from .04% to .16%. Transition Reynolds number dropped from 2.3×10^6 to 1.5×10^6. It appears, therefore, that the honeycomb was a much better turbulence damping mechanism than screens, with many screens being required to give the same reduction in turbulence as one honeycomb.

APPENDIX II

ACOUSTICS OF THE TEST SECTION

We wished to generate two-dimensional, plane, progressive sound waves in the test section, since this was both a simple sound field and one which was likely to occur in actual practice. Unfortunately, it was very difficult to generate plane progressive waves in a finite length duct, and some compromise had to be accepted. The two major sources of problems were reflections from the open end of the duct and reflections from the side walls of the duct. The former resulted in standing waves, giving longitudinal sound pressure variations, while the latter generated transverse and vertical variations by exciting higher order modes of the duct, as described in Morse and Ingard (1968).

The cutoff frequency for a rectangular cross-section duct is given by $f = c/2\ell$, where c is the speed of sound and ℓ is the duct width. The cutoff frequency is that frequency below which no transverse, higher order modes of sound propagation exist, so that only plane waves will propagate in the duct. Our duct had a 450 Hz cutoff and we were working in the frequency range from 500 Hz to 2000 Hz, so there were transverse modes of propagation

and therefore transverse variations in sound pressure. Longitudinal reflections from the open end of the duct occurred because of the change in acoustic impedance, exactly analogous to the reflections occurring in electrical circuits when there are impedance mismatches. Reflections would occur unless the sound wavelength was several times smaller than the duct dimension. The test section width was 38 cm, corresponding to the wavelength of a 900 Hz sound wave, so longitudinal reflections were also significant in the frequency range of interest, and testing was required.

The first test procedure used was to place a speaker in front of the wind tunnel entrance. The speaker was driven by white noise, with a flat frequency spectrum, and the response was picked up by a microphone in the test section. A spectrum analysis was done on the microphone signal using a real-time analyzer. This was a rapid test procedure which gave information over a wide frequency range. The first condition evaluated was a closed duct configuration, with the existing formica duct walls. This showed tremendous peaks and nulls of frequency response, with similarly large variation of up to 20 dB as the microphone position was varied. These early tests were done with and without flow through the tunnel, and showed

very little qualitative change, so subsequent tests were done without flow to simplify the procedure. The first modification was to change to an open-duct test configuration. This was somewhat improved, but still far from suitable. The test section walls were then lined with a thick fiberglass blanket material to prevent transverse reflections. This worked very well at reducing transverse pressure variations, but introduced a longitudinal attenuation of the order of 35 dB/meter. A scale model of the tunnel was built using an existing fiberglass model of the contraction. This was tested to further confirm the results, and dismiss the possibility of structural contributions to the problem. An open-duct test section was built with an acoustic lining on the walls. The foam used (an energy absorbing foam, donated by E-A-R Corp, Westwood, Mass.) was selected because it had only a moderate acoustic absorption coefficient, to reduce the longitudinal attenuation discussed above, and because its surface was extremely smooth, to avoid flow disturbances and noise generation.

This test section generally worked well. As the actual experiments progressed, however, it became clear that pure-tone excitation would be the dominant test condition rather than white noise. At this point, very

careful measurements were made. A loud pure tone was generated by the speaker in front of the tunnel while the tunnel was running at test speed, and the hot wire anemometer was used to measure the sound velocity levels, which were converted to sound pressure levels using the plane wave assumption (p. 31). A microphone was used to examine transverse variations, and as a check of the hot wire calibration. Loud sound, over 100 dB SPL, was used to overcome the wind noise on the microphone. The levels measured by the hot wire and the microphone agreed within $\pm$2 dB. Typical results gave a maximum variation of 4 dB in the sound pressure level at various test section locations, with a noticeable longitudinal standing wave. The reflection coefficient from the open end of the duct was estimated at 0.2, meaning that the reflected wave traveling upstream had an amplitude which was 0.2 of the amplitude of the downstream traveling incident wave. An "acoustic impedance transformer" was then added to the downstream end of the duct. This consisted of tapered wedges extending each wall of the duct, so that the walls ended more gradually. This reduced the reflection coefficient to 0.1, considered an acceptable level. Figure 11 shows the typical longitudinal variation in sound pressure level.

careful measurements were made. A loud pure tone was generated by the speaker in front of the tunnel while the tunnel was running at test speed, and the hot wire anemometer was used to measure the sound velocity levels. A microphone was used to examine transverse variations, and as a check of the hot wire calibration. Typical results gave a maximum variation of 4 dB in the sound pressure level at various test section locations, with a noticeable longitudinal standing wave. The reflection coefficient from the open end of the duct was estimated at 0.2, meaning that the reflected wave traveling upstream had an amplitude which was 0.2 of the amplitude of the downstream traveling incident wave. An "acoustic impedance transformer" was then added to the downstream end of the duct. This consisted of tapered wedges extending each wall of the duct, so that the walls ended more gradually. This reduced the reflection coefficient to 0.1, considered an acceptable level. Figure 11 shows the typical longitudinal variation in sound pressure level.

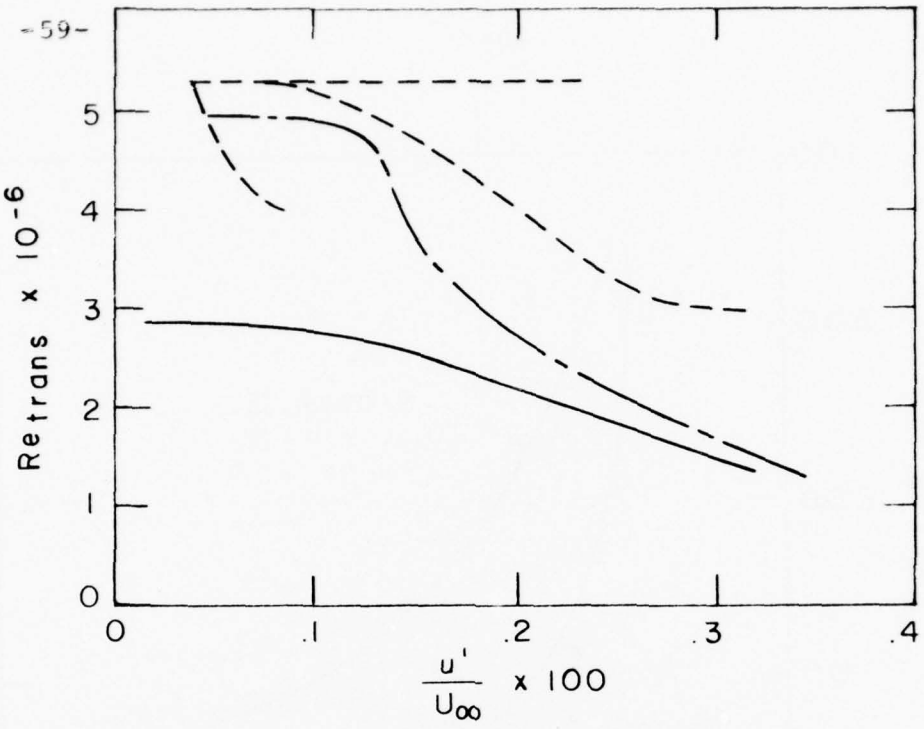

——— Schubauer and Skramstad (1948) results

—·—·— Increased turbulence generated by screens

– – – – Acoustic disturbances, of different frequencies

EFFECT OF VARIOUS FREE-STREAM DISTURBANCES ON THE TRANSITION REYNOLDS NUMBER

Taken from Spangler and Wells (1968).

FIGURE 1

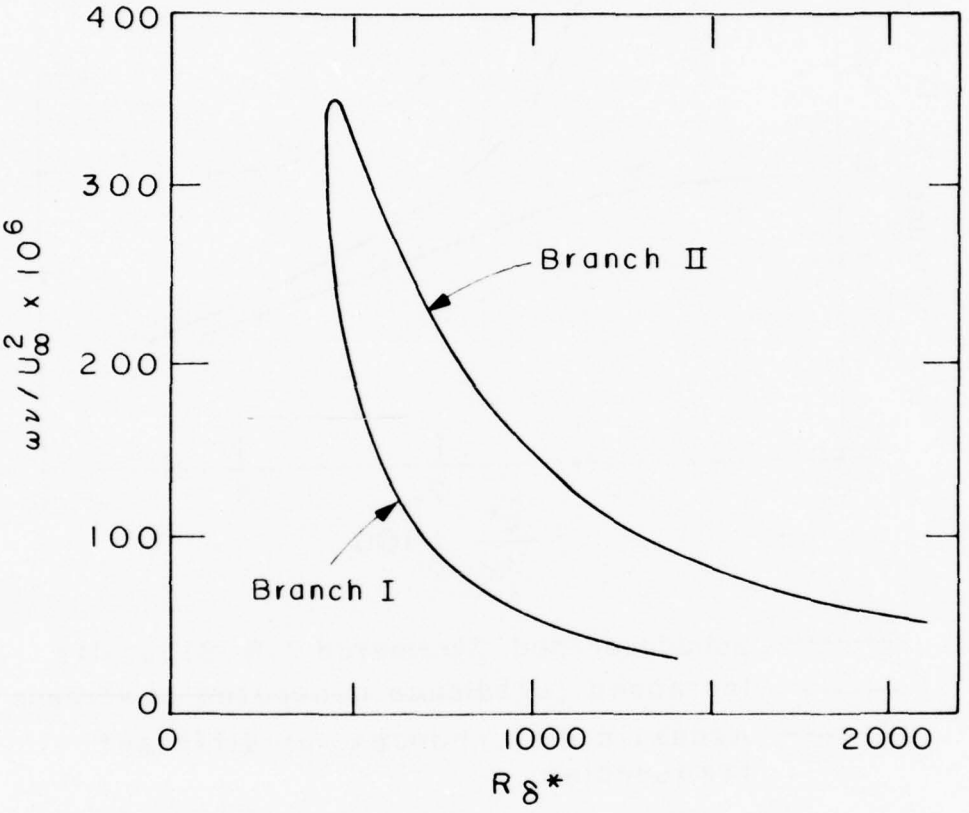

NEUTRAL STABILITY CURVE, FLAT PLATE, ZERO PRESSURE GRADIENT.

Taken from Shen (1954)

FIGURE 2

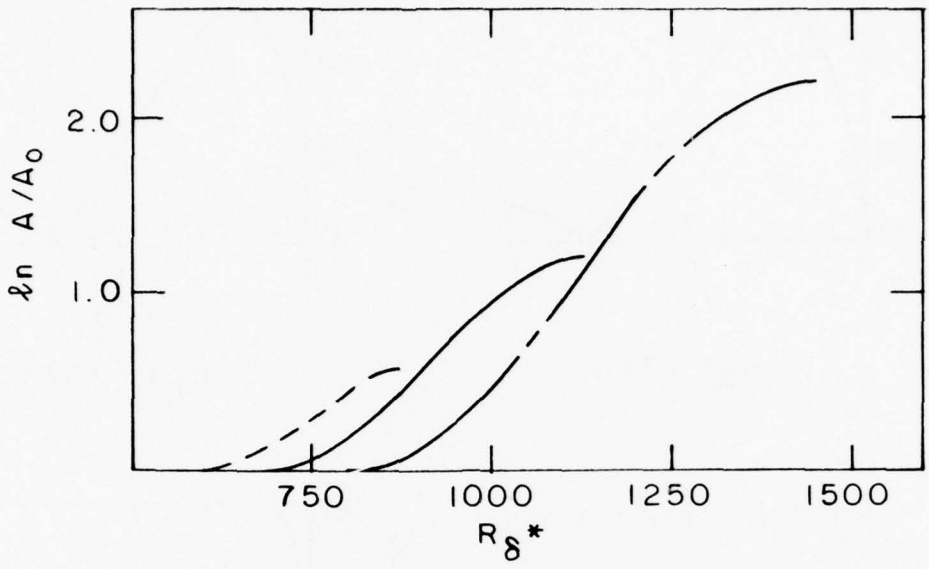

– – – – $\beta_r = \frac{\omega \nu}{U_\infty^2} = 157 \times 10^{-6}$

——— $\beta r = 110 \times 10^{-6}$

— — — $\beta r = 82 \times 10^{-6}$

THEORETICAL SPATIAL GROWTH CURVES FOR SEVERAL FREQUENCIES

Taken from Ross, Barnes, Burns and Ross (1970)

FIGURE 3

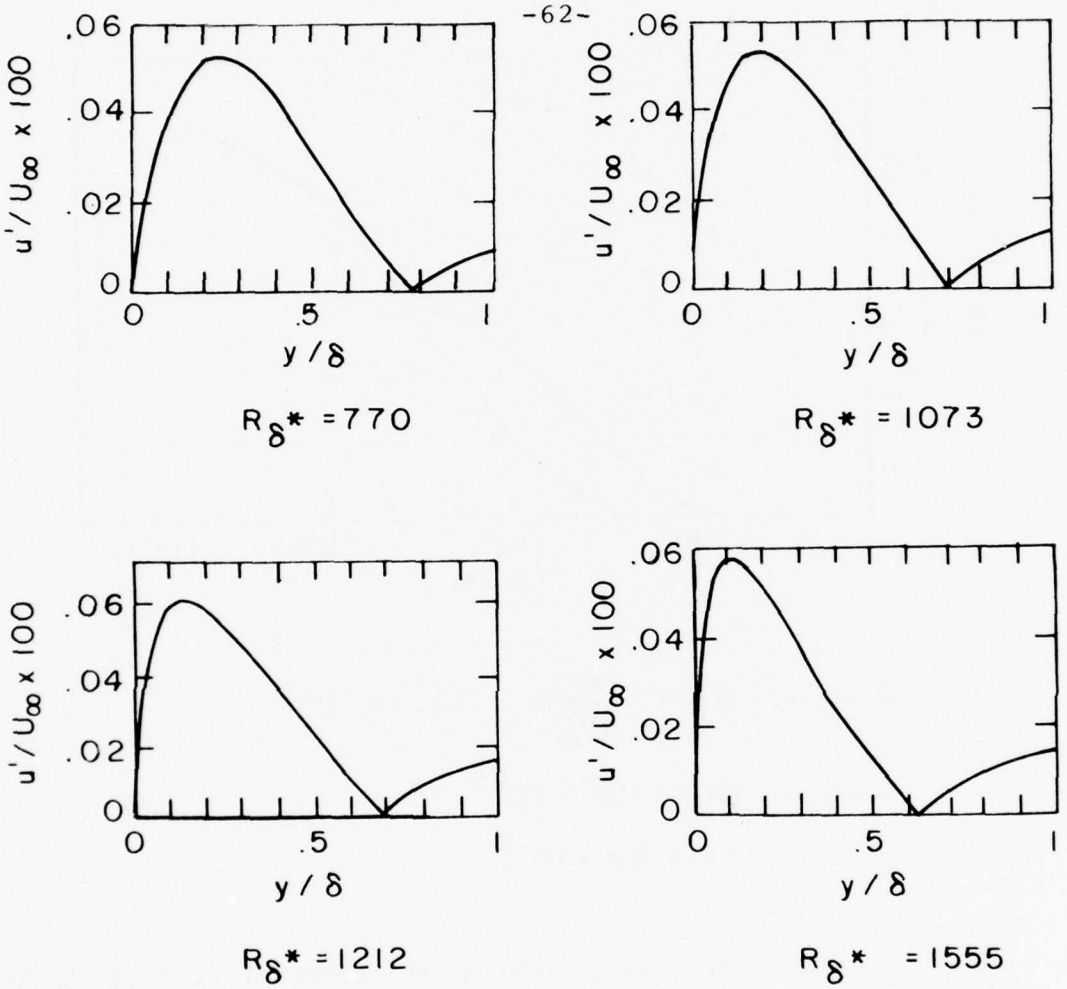

THEORETICAL CURVES OF TOLLMIEN-SCHLICHTING WAVE AMPLITUDE VS. y/δ FOR $\beta_r = \frac{\omega \nu}{U_\infty^2} = 82 \times 10^{-6}$, AT DIFFERENT R_δ^*.

Taken from Ross, Barnes, Burns and Ross (1970)

FIGURE 4

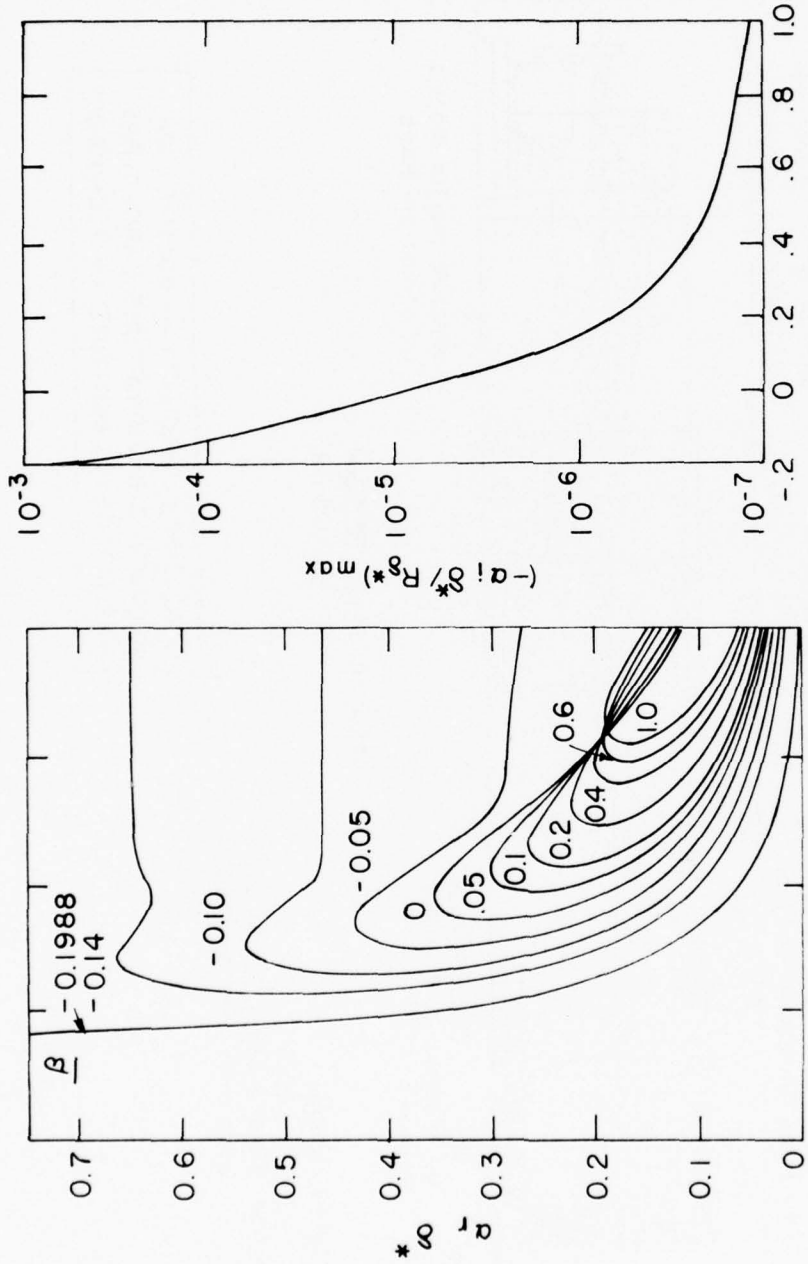

NEUTRAL STABILITY CURVES FOR VARIOUS VALUES OF THE FALKNER-SCAN PARAMETER, β.

EFFECT OF PRESSURE GRADIENT ON THE MAXIMUM SPATIAL AMPLIFICATION RATE.

Taken from Obremski, Morkovin, and Landahl (1969)

FIGURE 5

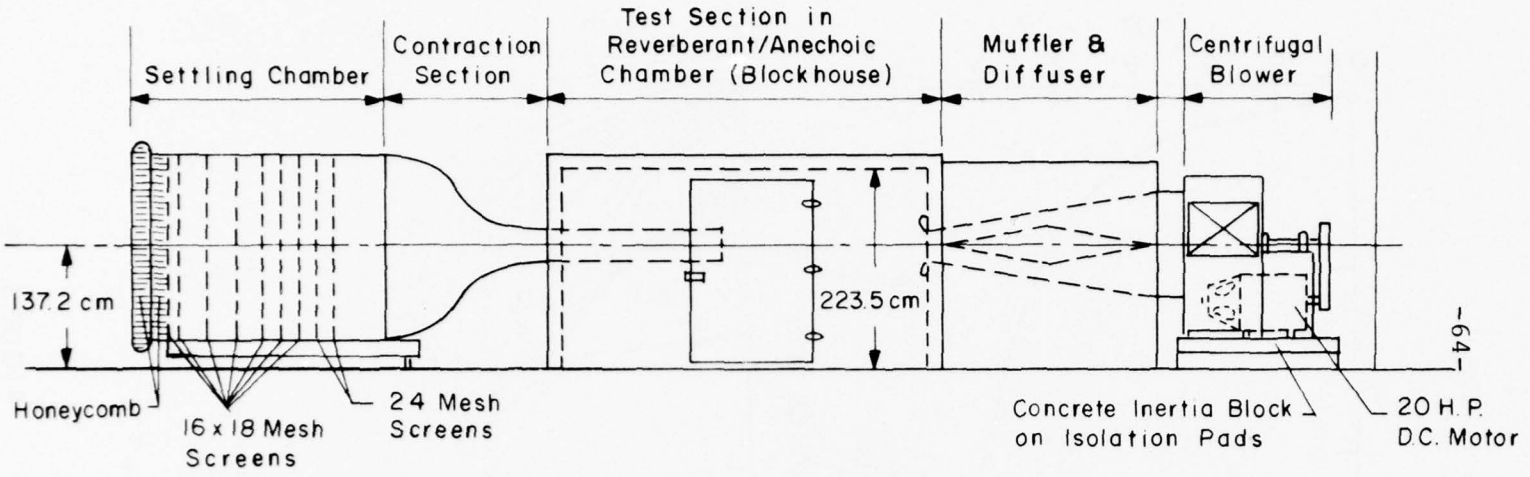

FIGURE 6

General Specifications:
Contraction Ratio: 20:1
Test Section: 38cm x 38cm, shown in open duct configuration

WIND TUNNEL FACILITY — ROOM 5-024
ACOUSTICS & VIBRATIONS LABORATORY
MASSACHUSETTS INSTITUTE OF TECHNOLOGY

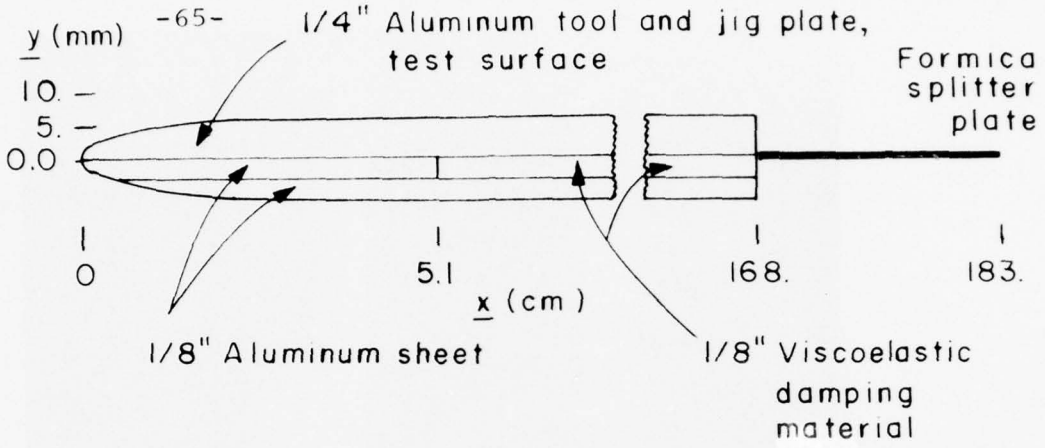

ELEVATION VIEW OF TEST PLATE

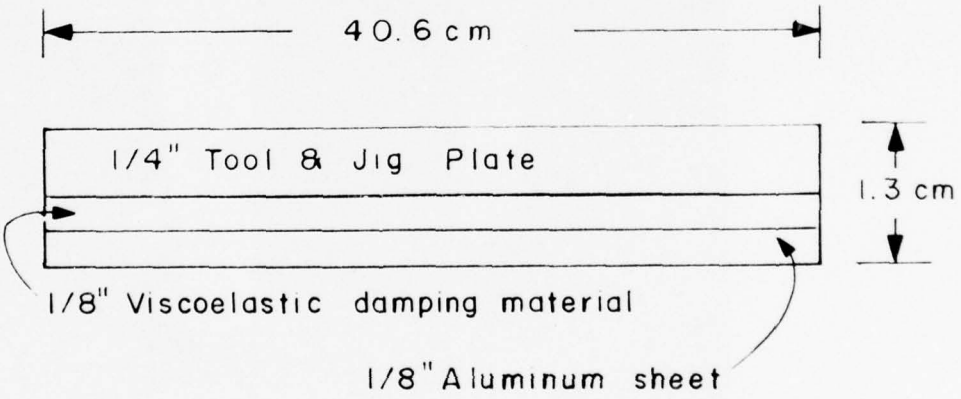

CROSS-SECTIONAL VIEW OF TEST PLATE

TEST PLATE CONSTRUCTION

FIGURE 7

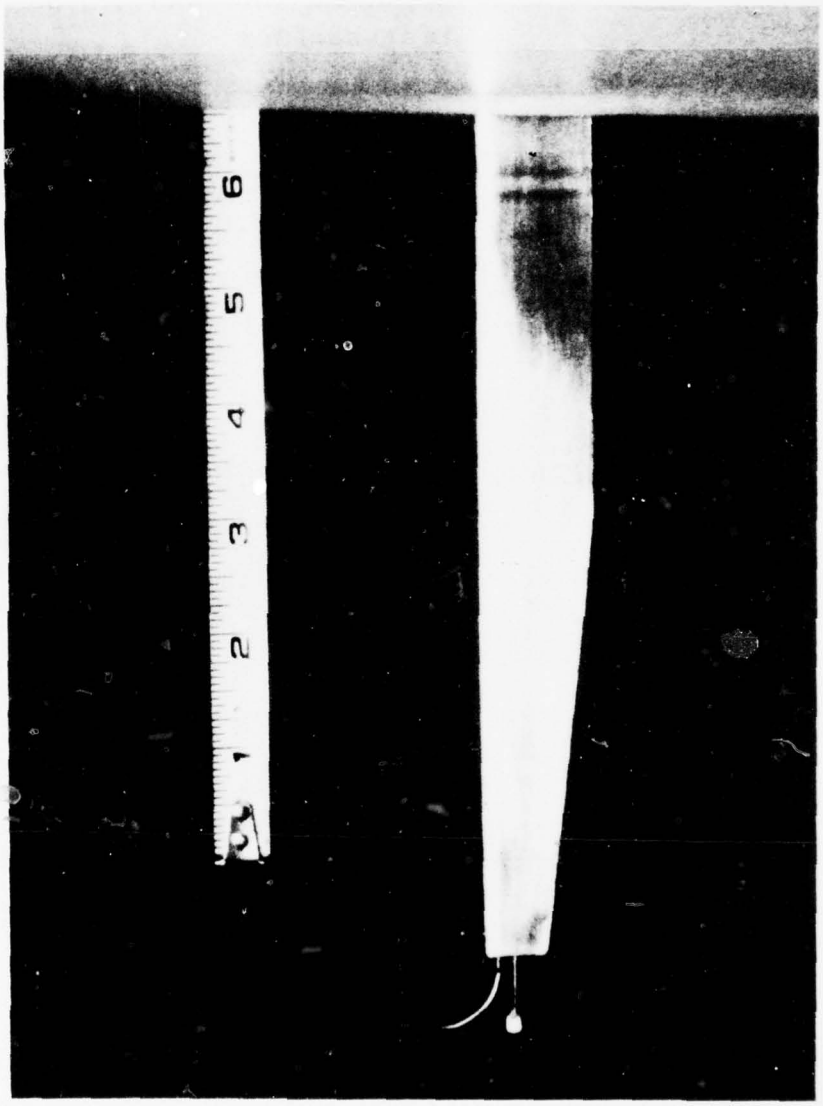

TRAVERSE WITH HOT-WIRE PROBE INSTALLED

FIGURE 8

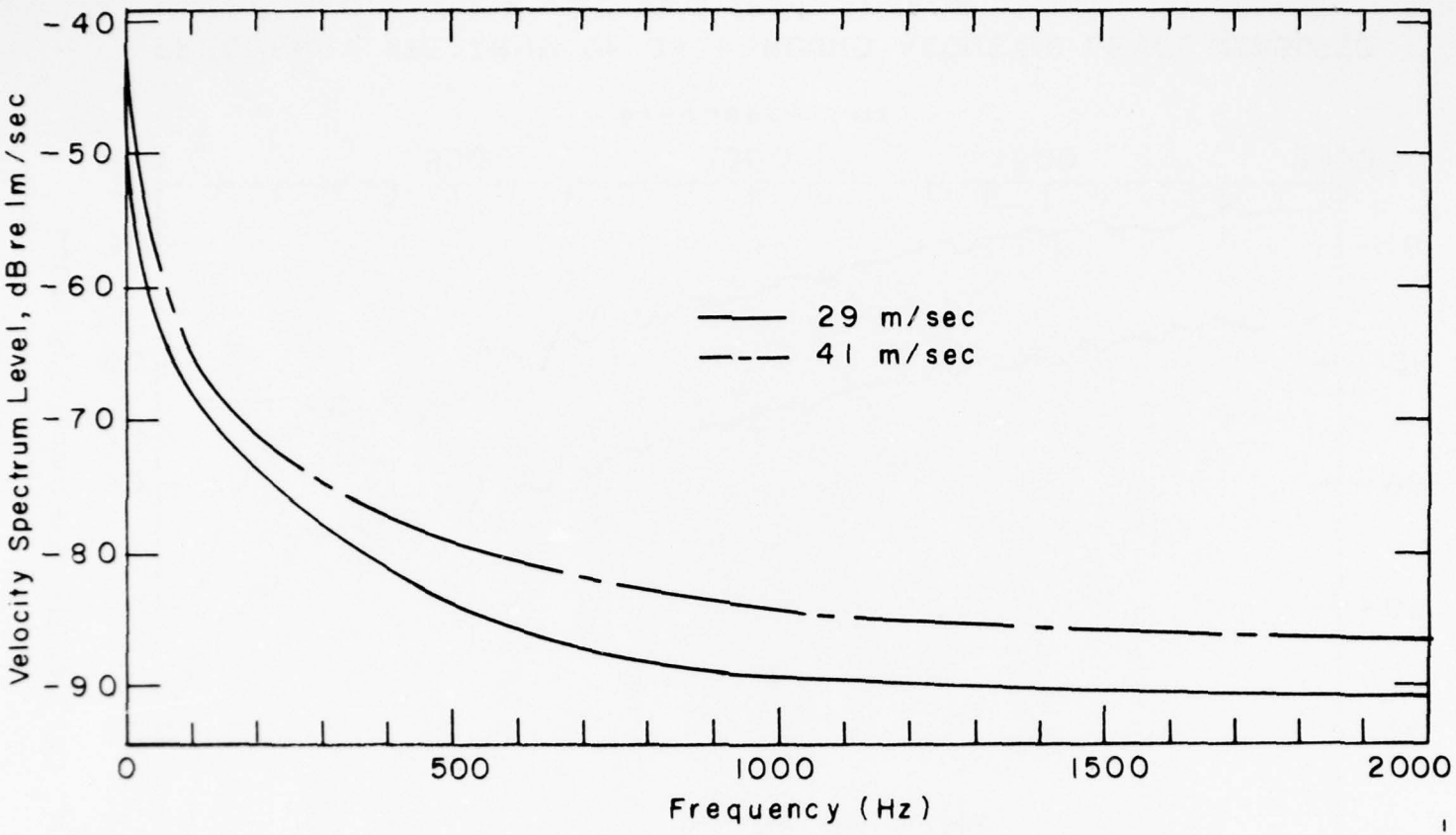

FIGURE 9

For frequencies greater than 1000 Hz, the signal is obscured by the anemometer noise.

FREQUENCY SPECTRUM OF FREE-STREAM TURBULENCE AT TWO TEST SPEEDS

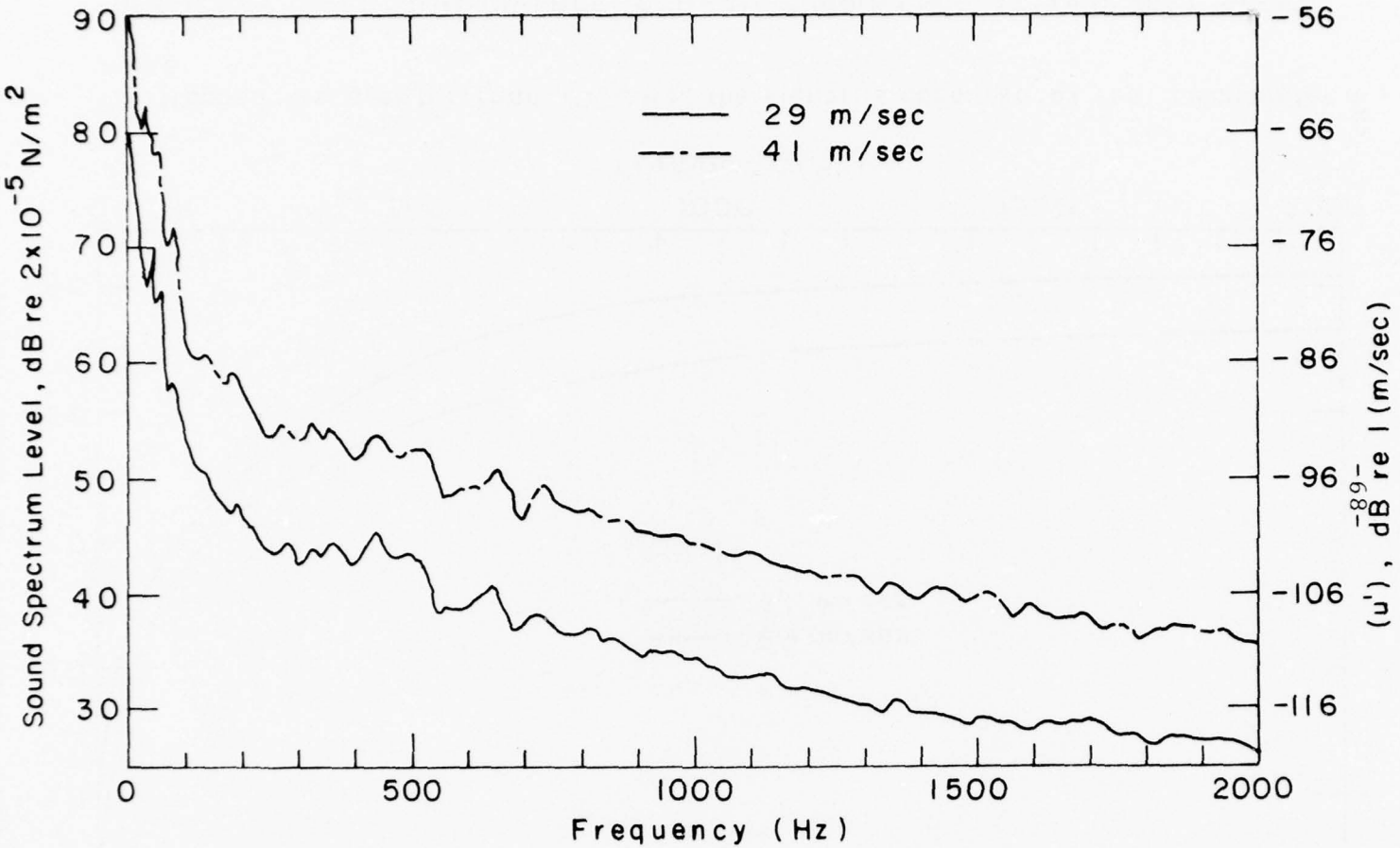

FIGURE 10

FREQUENCY SPECTRUM OF BACKGROUND ACOUSTIC LEVEL MEASURED IN THE BLOCKHOUSE, AT TWO TEST SPEEDS

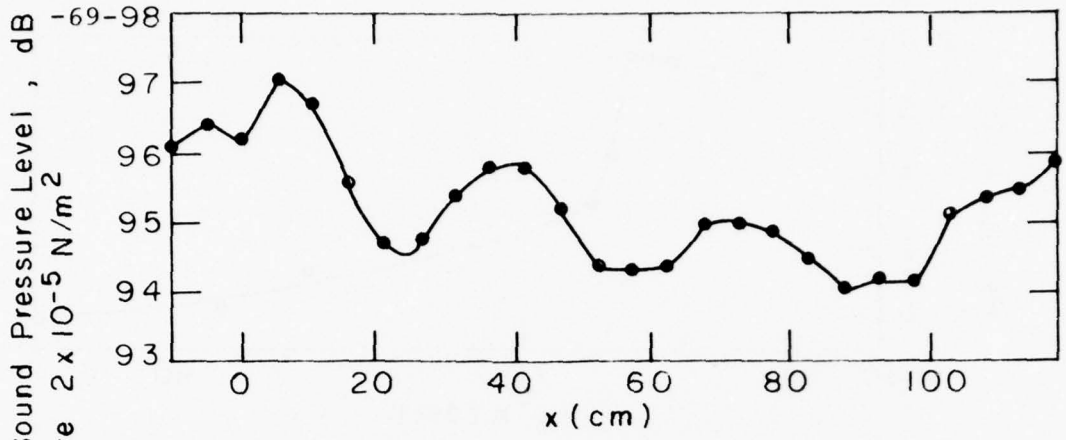

TEST SECTION ACOUSTIC LEVELS AT 29m/sec MEAN FLOW. 500Hz PURE TONE GENERATED BY LOUDSPEAKER AT TUNNEL ENTRANCE

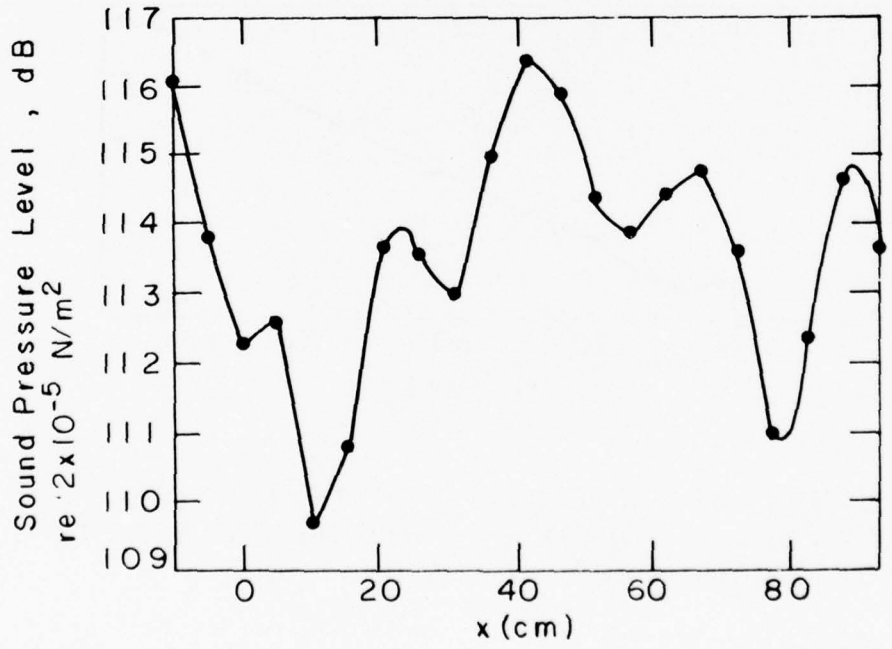

TEST SECTION ACOUSTIC LEVELS. U_∞ = 29m/sec, f = 1000Hz. LOUDSPEAKER AT TUNNEL ENTRANCE

FIGURE 11

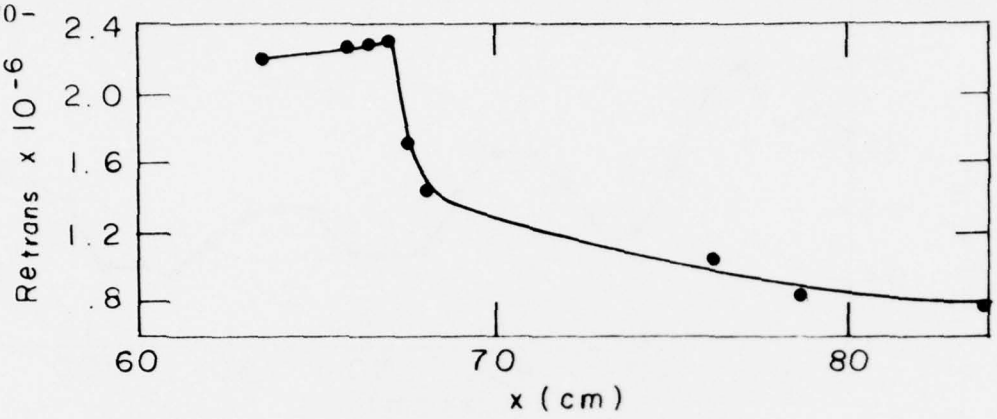

Distance from plate leading edge

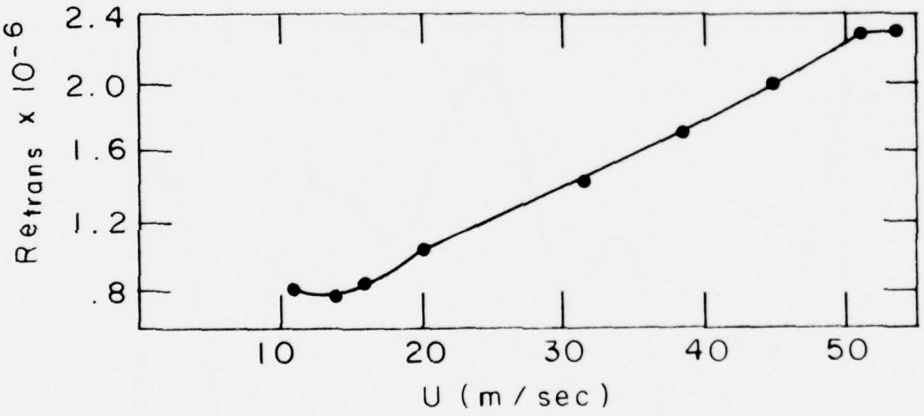

EARLY MEASUREMENTS OF TRANSITION REYNOLDS NUMBER, SHOWING THE EFFECTS OF TRANSVERSE CONTAMINATION

FIGURE 12

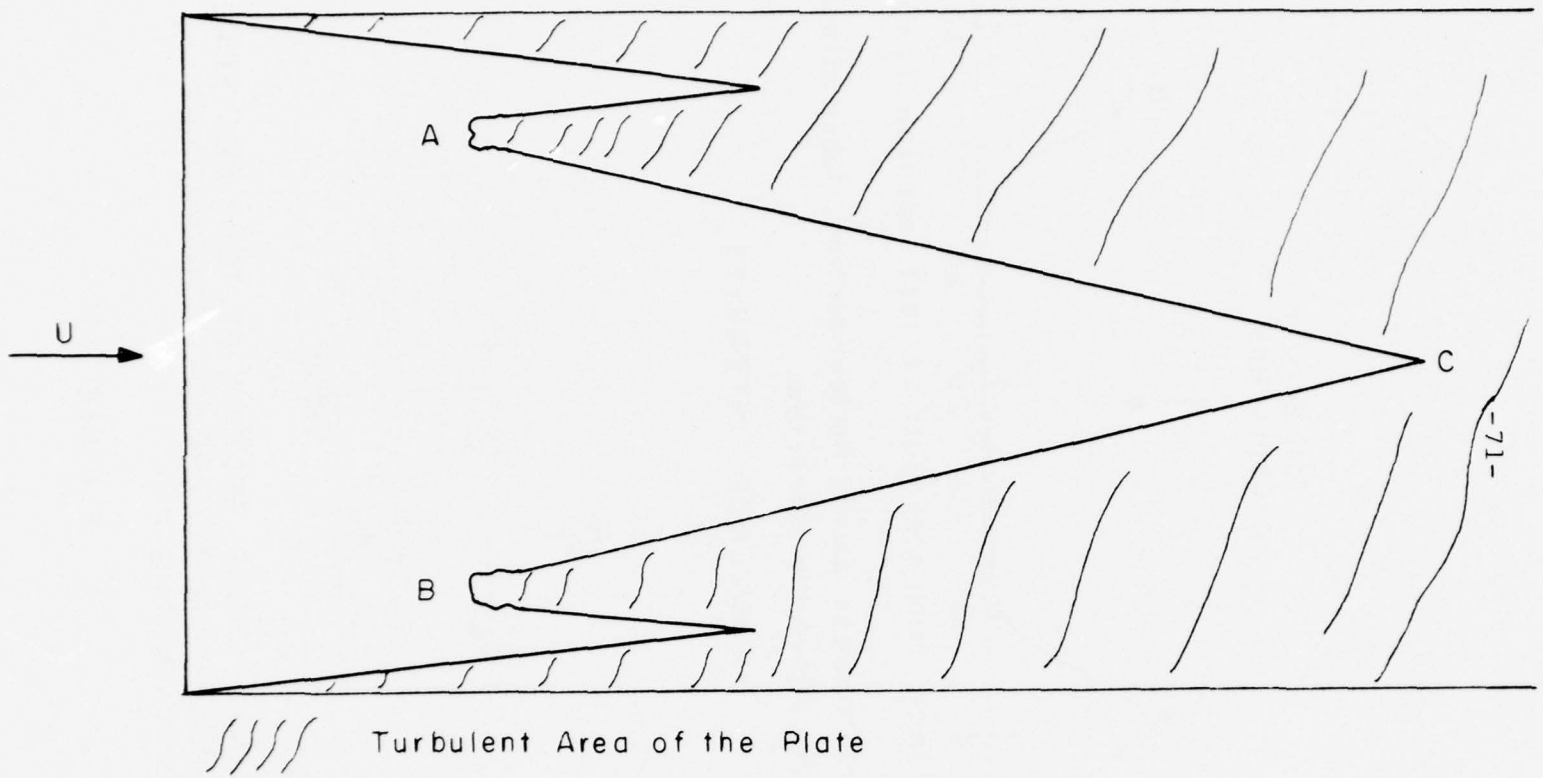

FIGURE 13

The wedge starting regions, A & B, move forward as the speed increases. This shifts the whole pattern forward, changing the location of the centerline transition point, C.

FLOW VISUALIZATION AT U ~ 30 m/sec

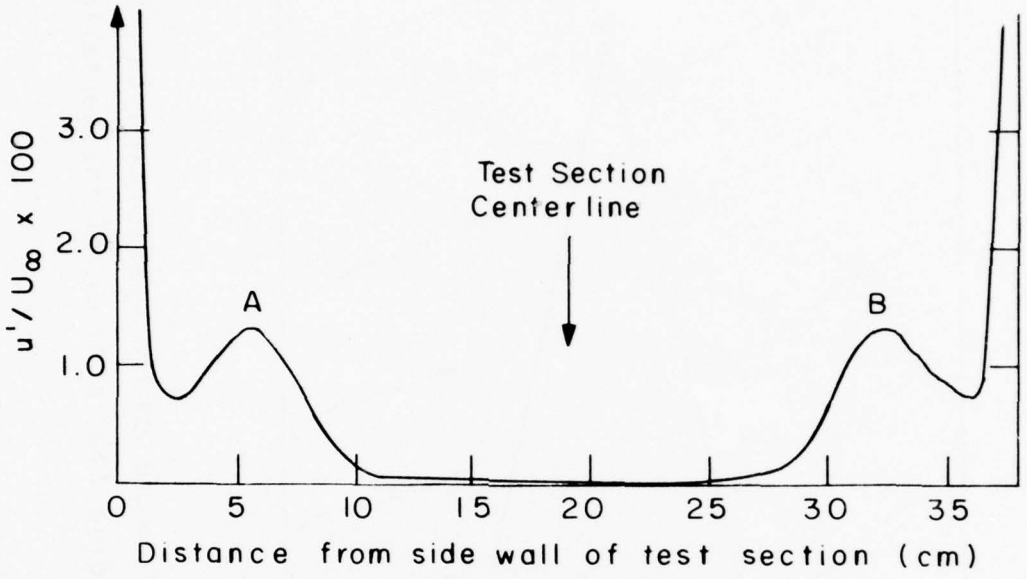

Horizontal traverse across the test section, taken with the probe 6 mm above the centerline.

TURBULENCE INTENSITY

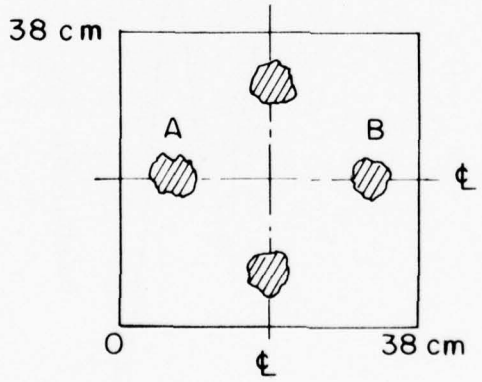

LONGITUDINAL CROSS-SECTION OF TEST SECTION, SHOWING APPROXIMATE AREAS OF INCREASED TURBULENCE INTENSITY

FIGURE 14

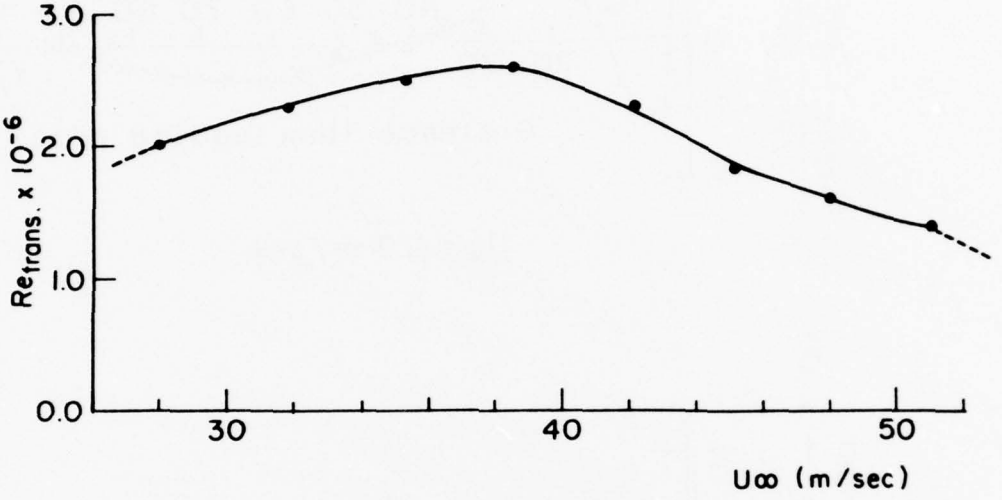

TRANSITION REYNOLDS NUMBER AT VARIOUS TUNNEL SPEEDS, FOR THE FINAL TEST FACILITY

FIGURE 15

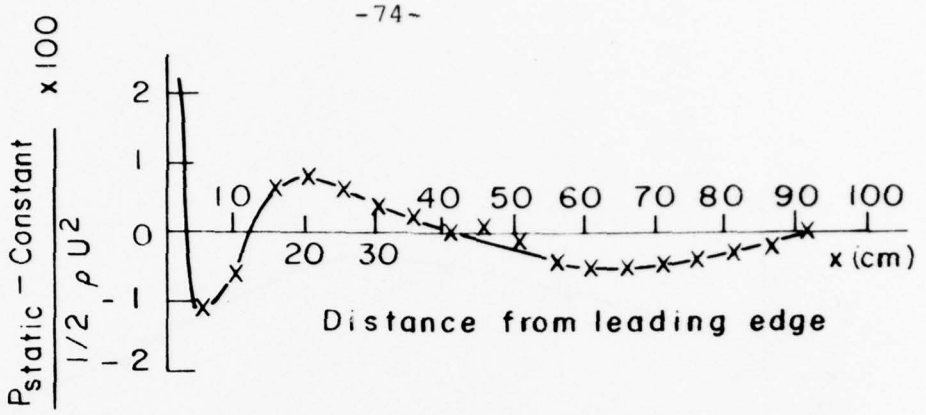

$U_\infty = 29$ m/sec

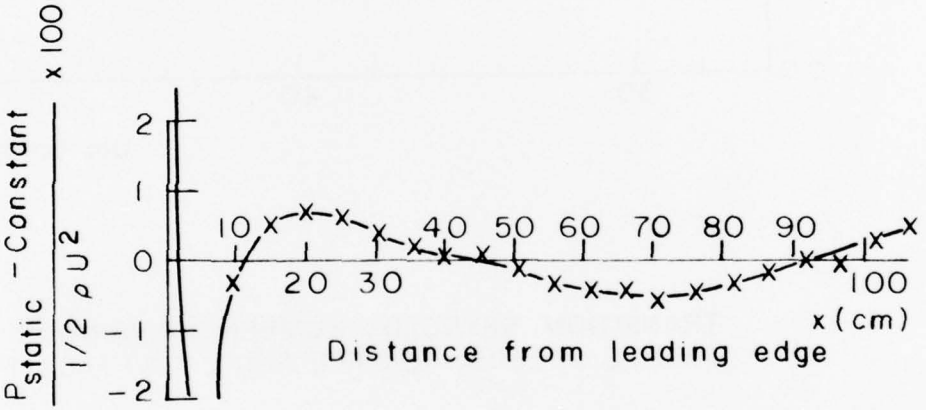

$U_\infty = 41$ m/sec

STATIC PRESSURE DISTRIBUTION

FIGURE 16

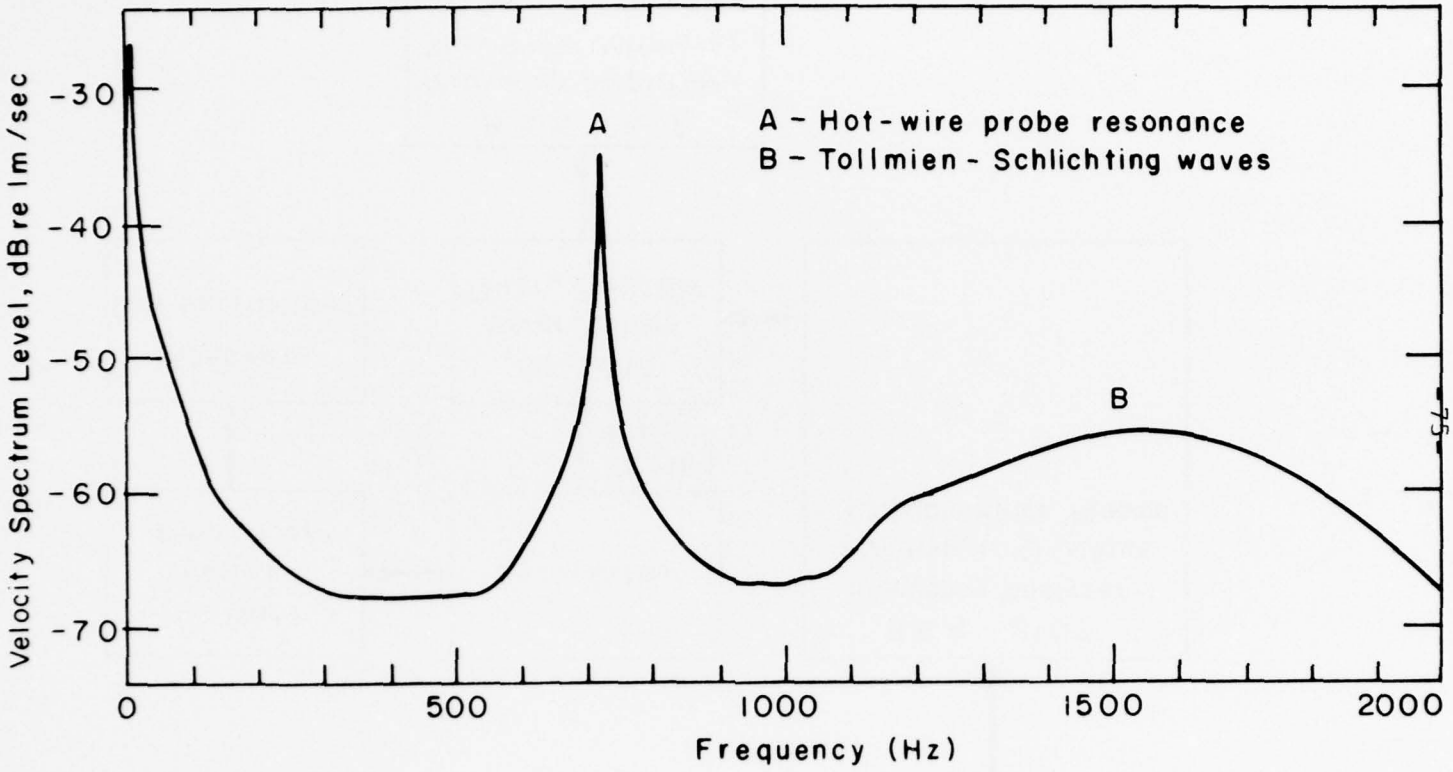

FIGURE 17

FREQUENCY SPECTRUM OF THE HOT-WIRE SIGNAL IN THE BOUNDARY LAYER. U_∞ = 41 m/sec, x = 21 cm, y = .4 mm.

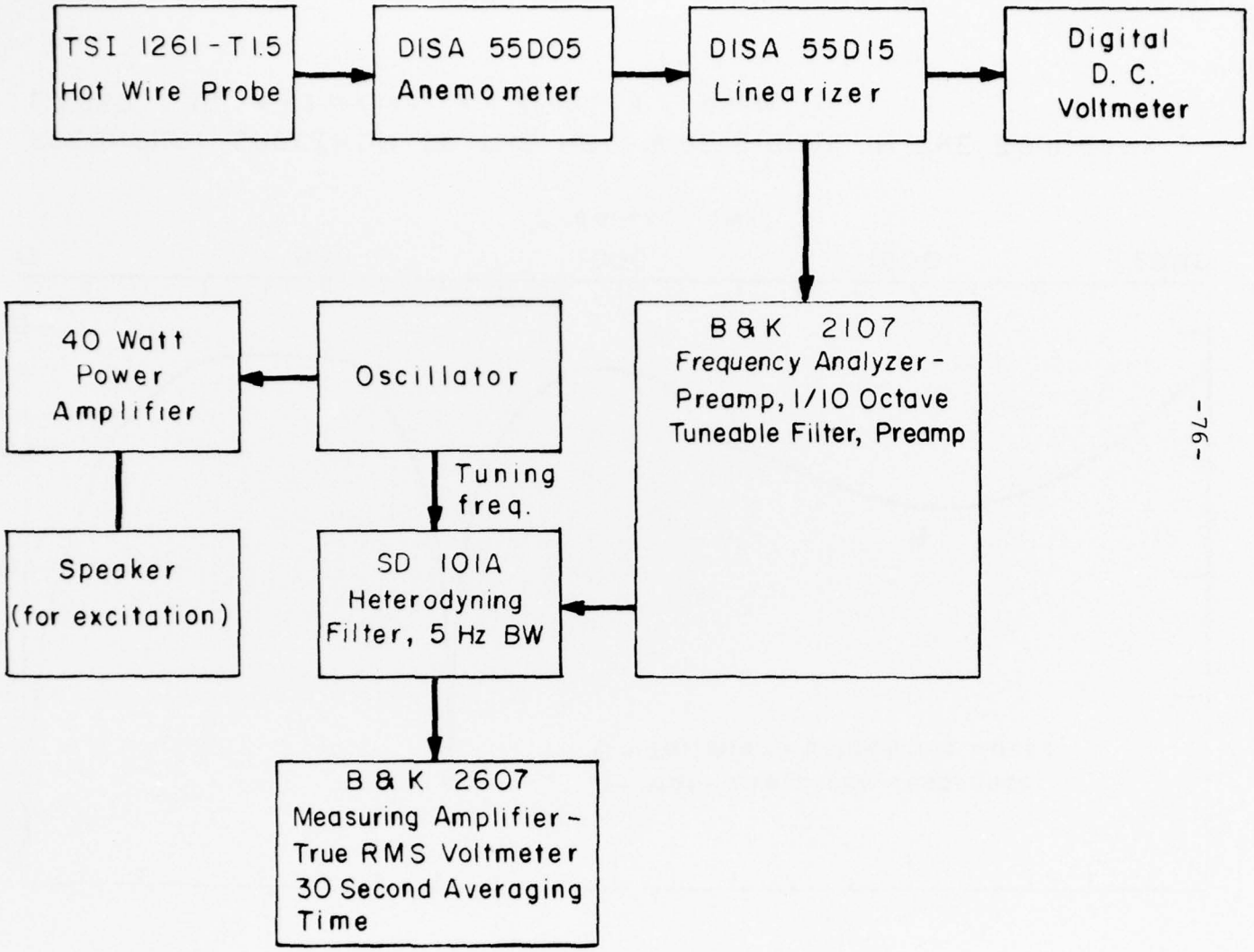

INSTRUMENTATION CHAIN

FIGURE 18

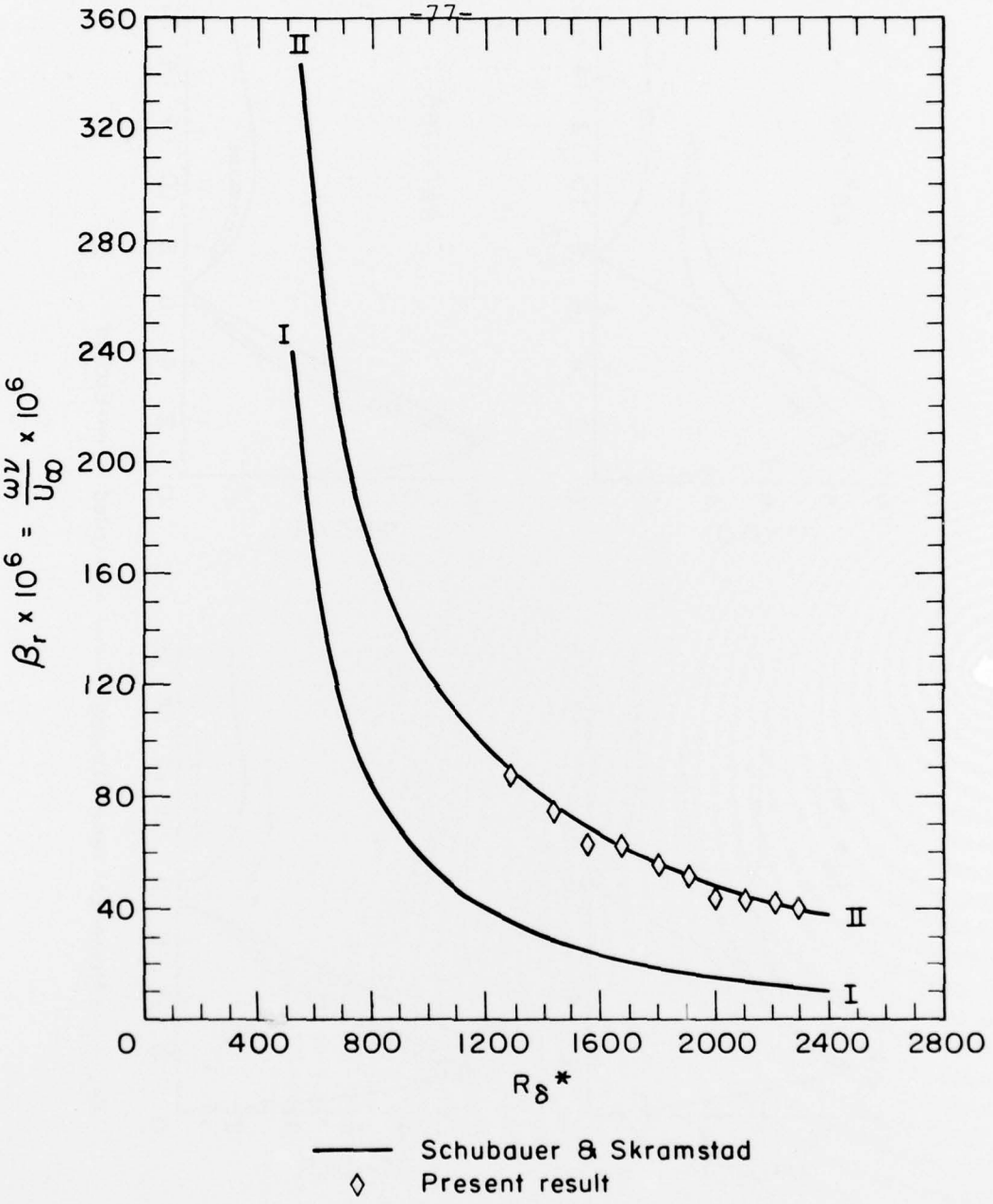

COMPARISON OF EXPERIMENTAL POINTS WITH NEUTRAL STABILITY CURVE FOUND EXPERIMENTALLY BY SCHUBAUER & SKRAMSTAD (1948)

FIGURE 19

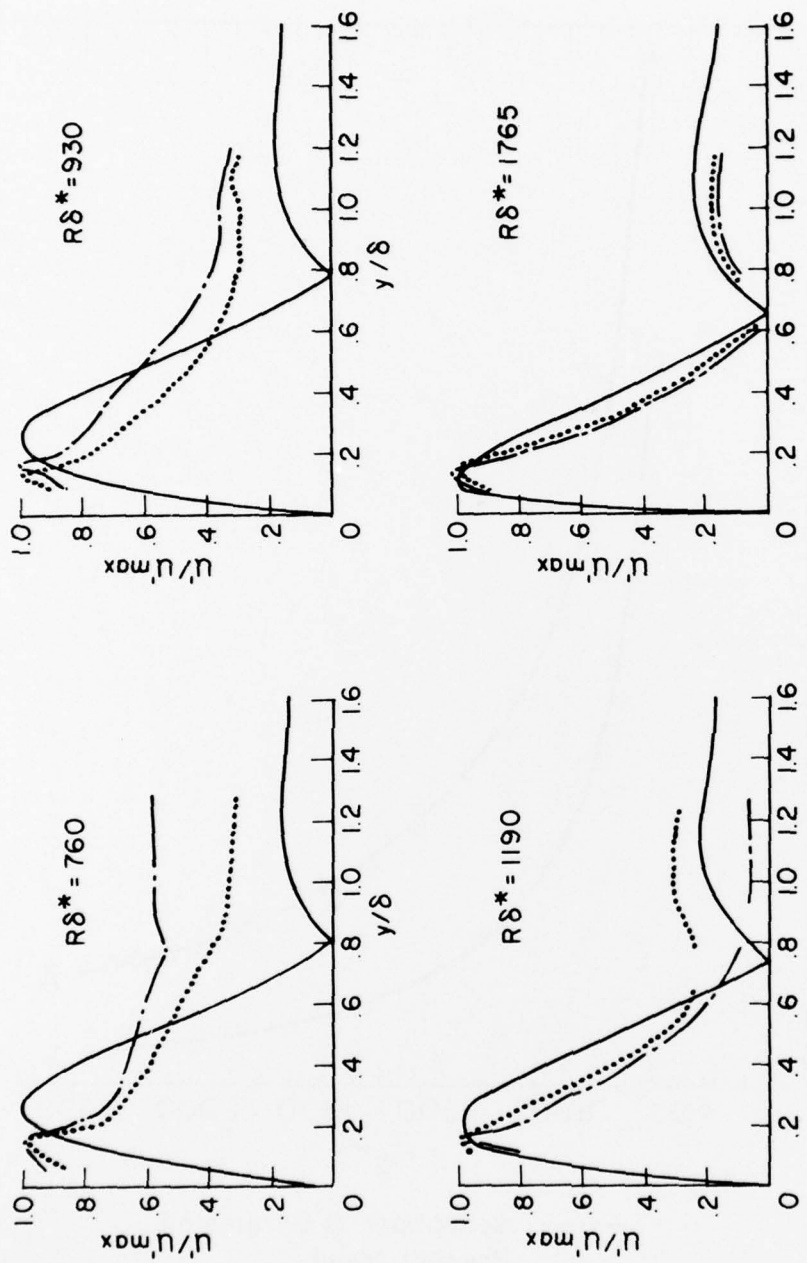

NORMALIZED TOLLMIEN-SCHLICHTING AMPLITUDE AS A FUNCTION OF y/δ^*, FOR SEVERAL VALUES OF $R\delta^*$; $\beta_r = 56 \times 10^{-6}$

FIGURE 20

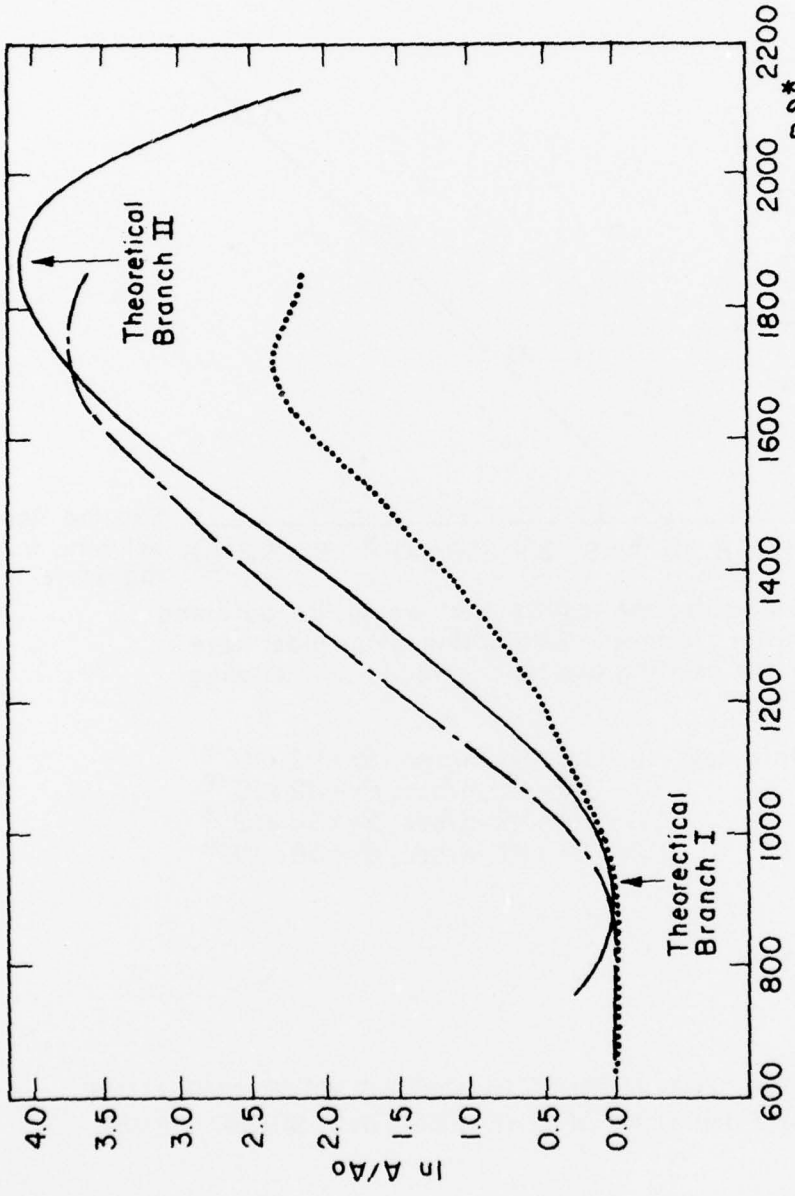

FAIRED TOLLMIEN-SCHLICHTING GROWTH CURVES

FIGURE 21

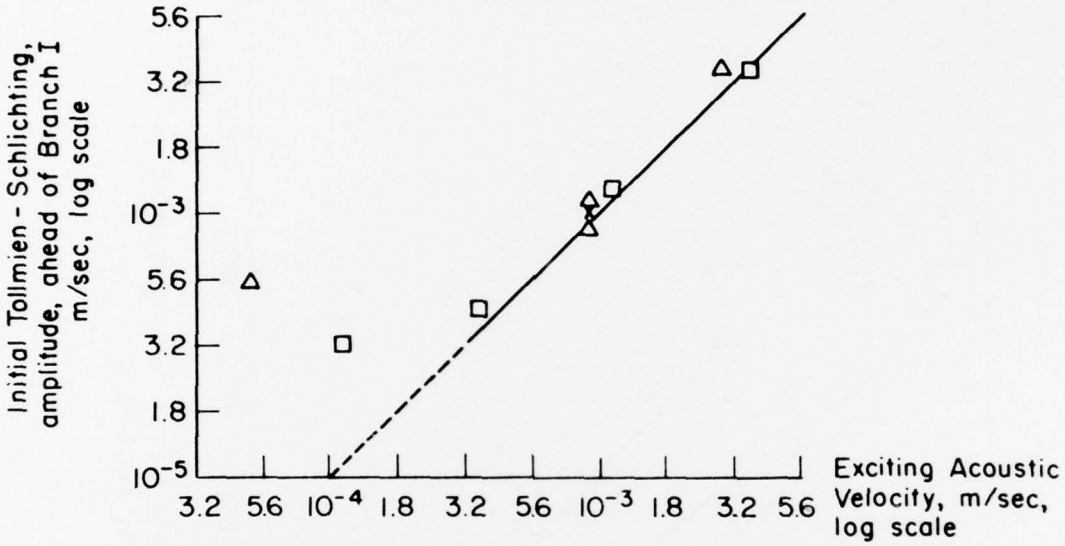

The line indicates the results that would be obtained if the initial Tollmien-Schlichting amplitude were equal to the exciting acoustic velocity (a coupling factor of 1.0).

Data Key:
- o - U_∞ = 41 m/sec, $\beta r = 112 \times 10^{-6}$
- x - U_∞ = 29 m/sec, $\beta r = 112 \times 10^{-6}$
- □ - U_∞ = 29 m/sec, $\beta r = 56 \times 10^{-6}$
- △ - U_∞ = 41 m/sec, $\beta r = 56 \times 10^{-6}$

INITIAL TOLLMIEN-SCHLICHTING WAVE AMPLITUDE AS A FUNCTION OF THE EXCITING SOUND LEVEL

FIGURE 22

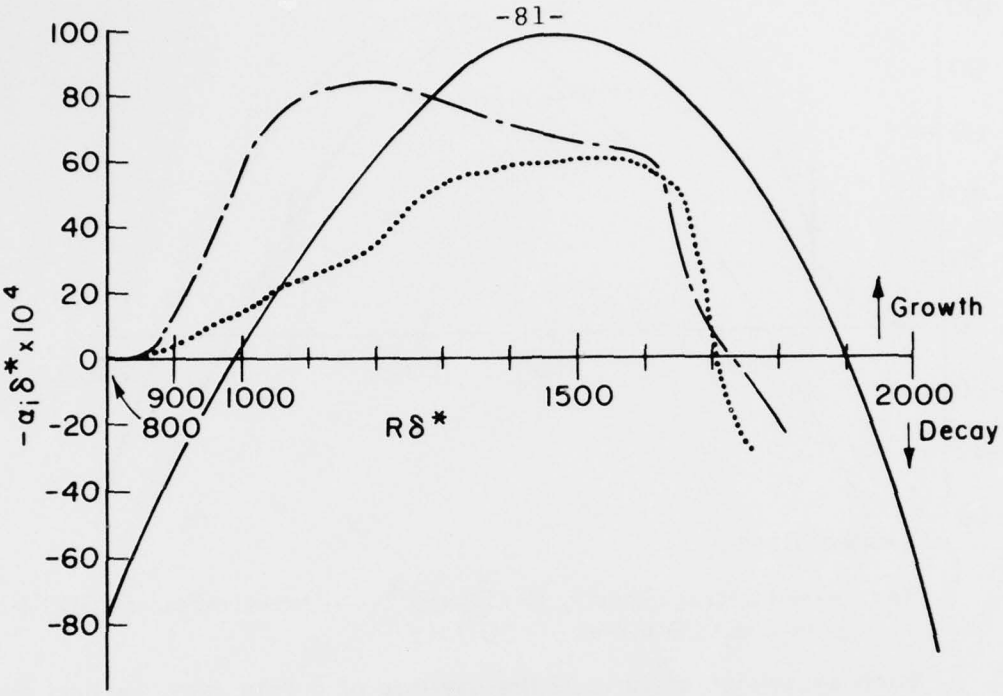

$\beta r = 56 \times 10^{-6}$, Same data as shown in Figure 21
Key: ——Theory (Orszag) ·····Unexcited
—·—Excited, 97 dB SPL

EXPERIMENTAL AND THEORETICAL TOLLMIEN-SCHLICHTING GROWTH RATES, $\alpha_i\delta^*$ vs. $R\delta^*$

FIGURE 23

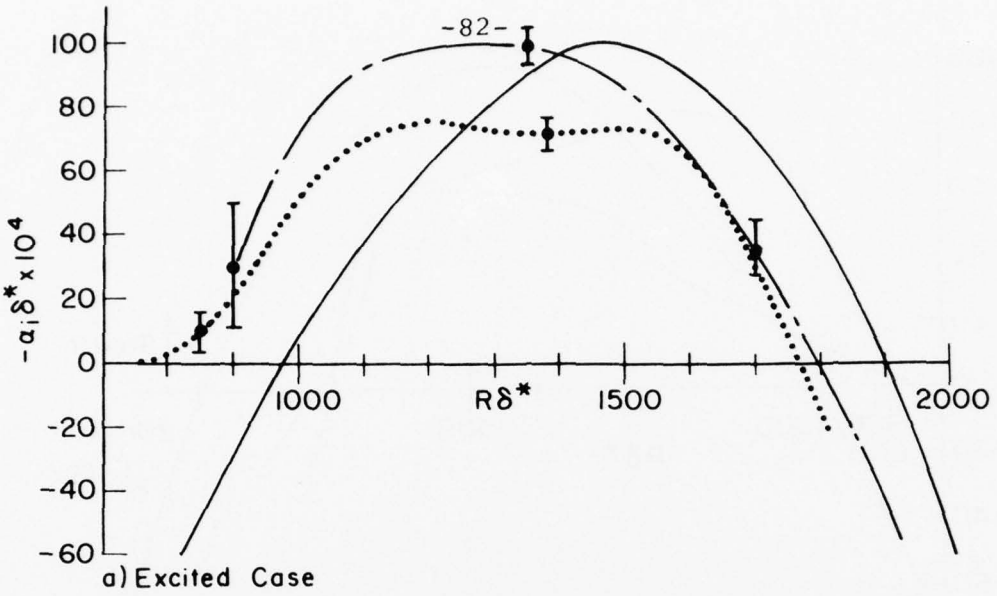

a) Excited Case

Key: ——(Orszag) Theory, $\beta r = 56 \times 10^{-6}$ ·——· $U\infty = 41$ m/sec, f = 1000 Hz
····· $U\infty = 29$ m/sec, f = 500 Hz

Each experimental curve is the average of 3 data runs. Vertical bars indicate the approximate deviation of the data.

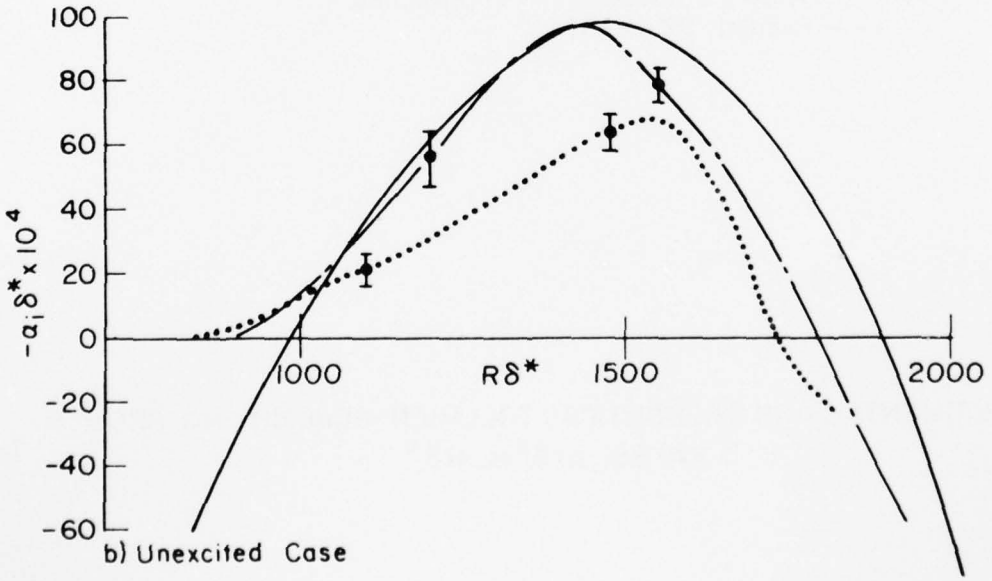

b) Unexcited Case

RESULTS AT TWO DIFFERENT TUNNEL SPEEDS, SHOWING A UNIT REYNOLDS NUMBER EFFECT.

FIGURE 24

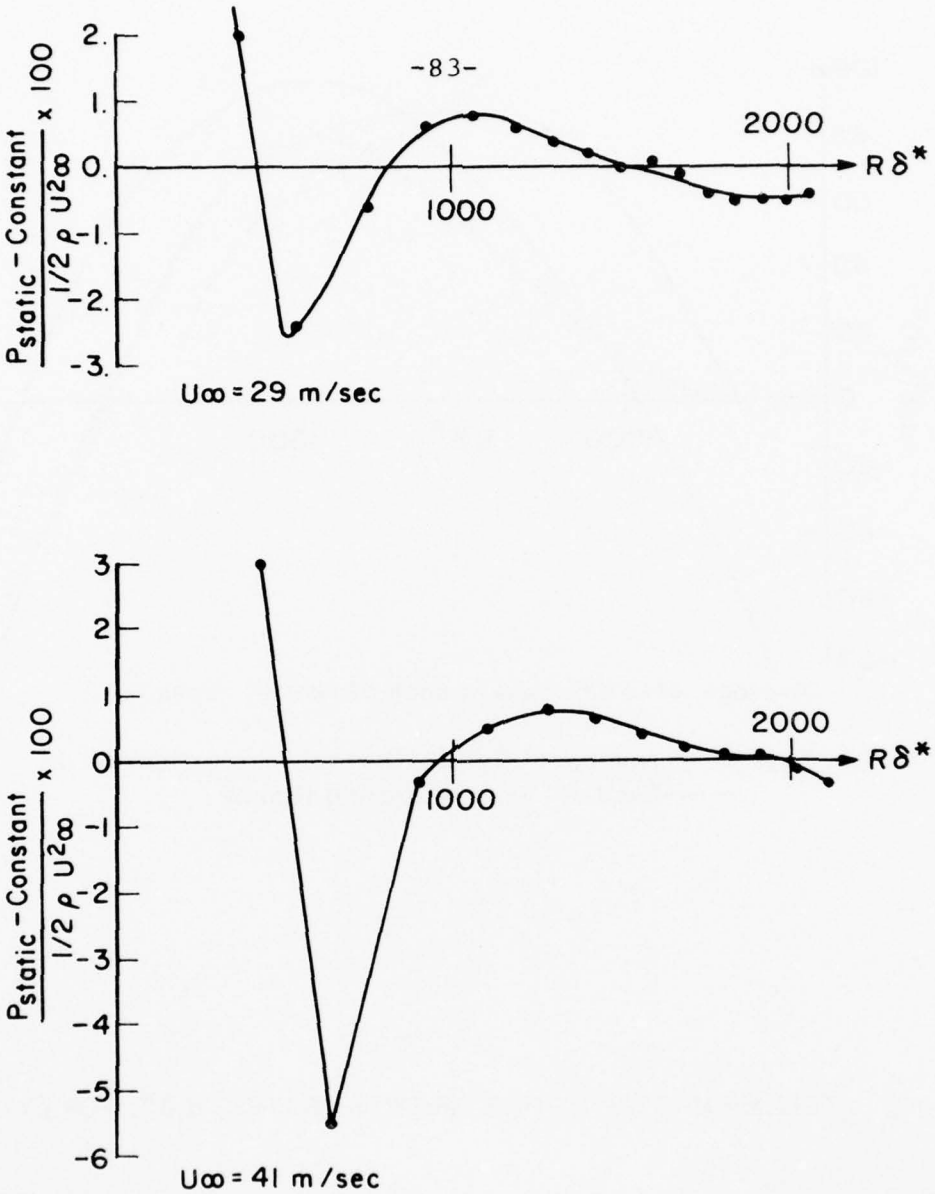

The pressure gradient is proportional to the derivates of these curves.

STATIC PRESSURE DISTRIBUTION AS A FUNCTION OF $R\delta^*$

FIGURE 25

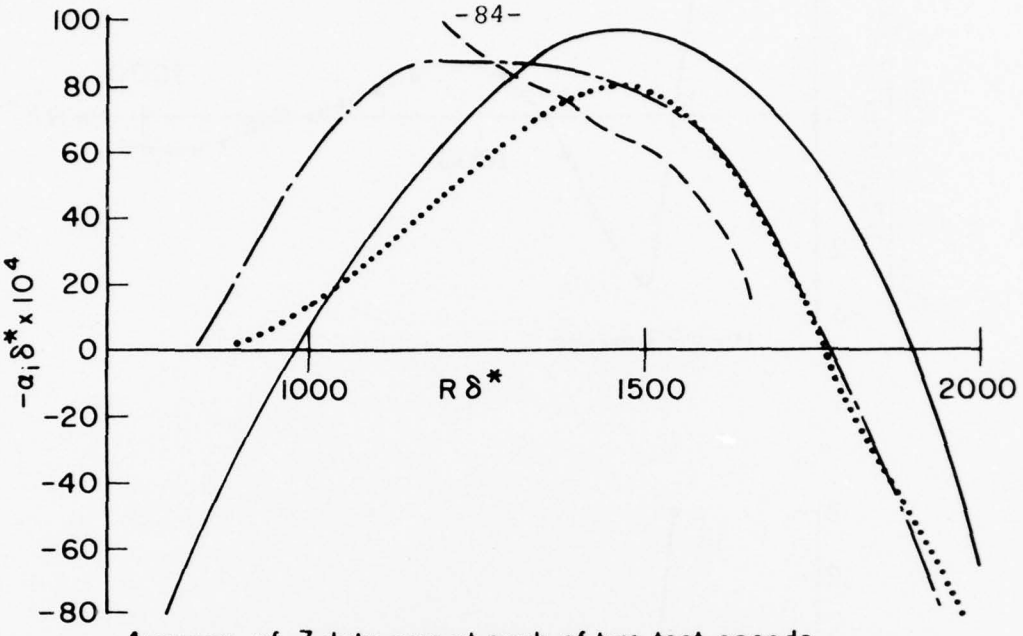

Average of 3 data runs at each of two test speeds.

Key: —— Numerical Result (Orszag) ·····Unexcited
—·—Excited ———Vibrating Ribbon

TOLLMIEN-SCHLICHTING GROWTH RATES, $\alpha_i\delta^*$, FOR $\beta r = 56 \times 10^{-6}$

FIGURE 26

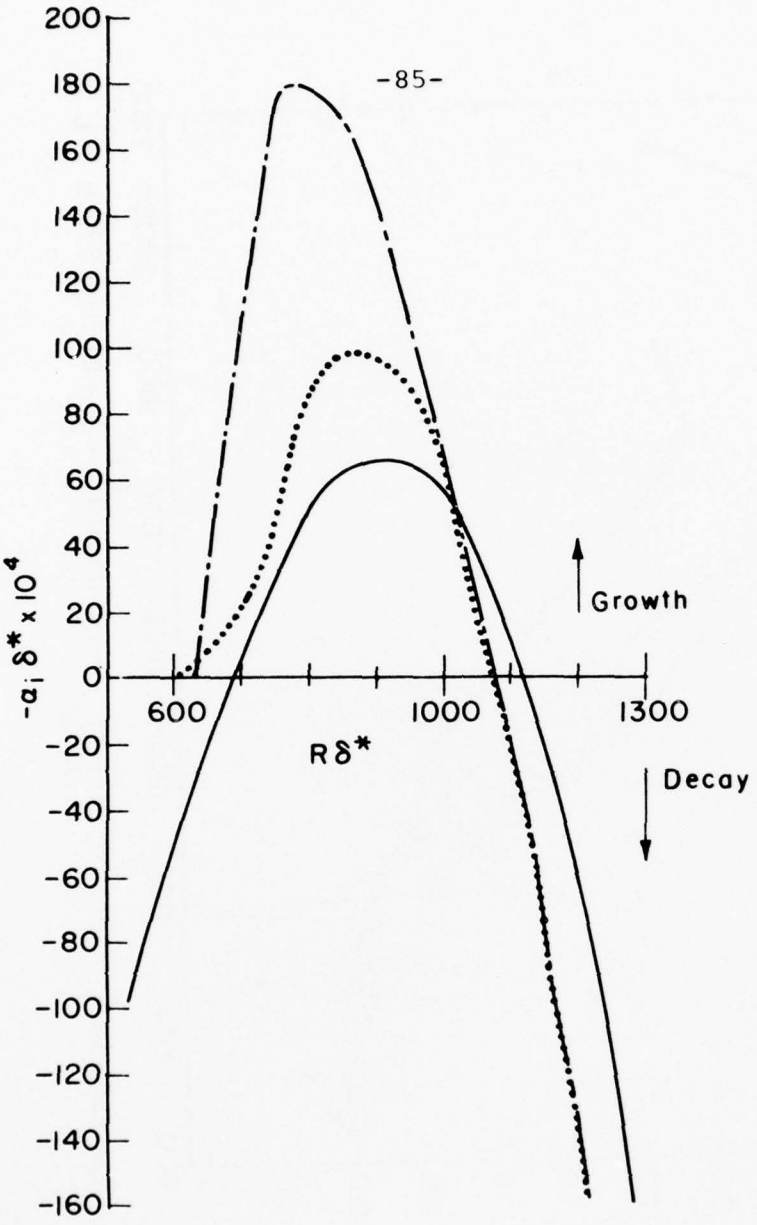

Key: ——Numerical Result (Orszag) ·····Unexcited —·—·—Excited

Average of 1 data run at each of two test speeds.

TOLLMIEN-SCHLICHTING GROWTH RATES, $\alpha_i \delta^*$, FOR $\beta r = 112 \times 10^{-6}$

FIGURE 27

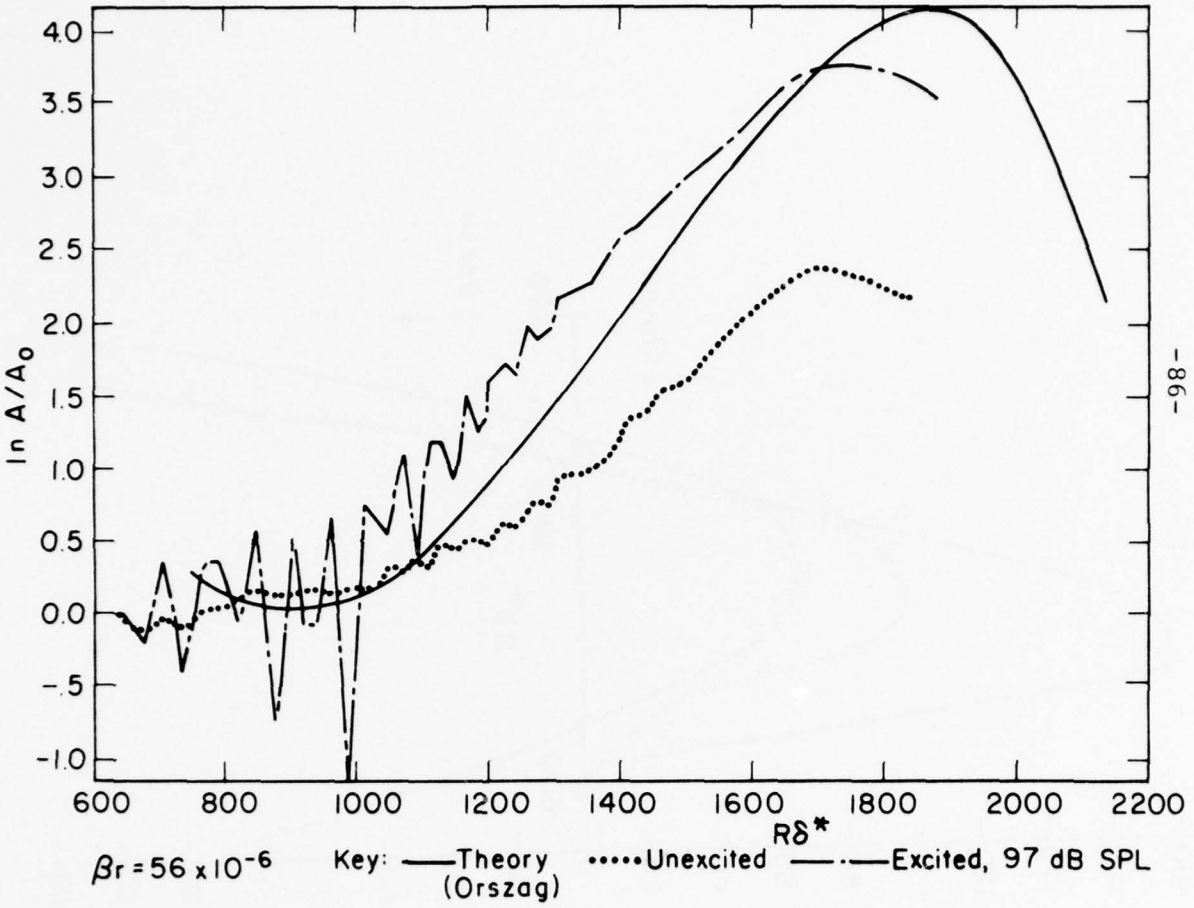

FIGURE 28

ACTUAL TOLLMIEN-SCHLICHTING GROWTH DATA
U∞ = 29 m/sec, f = 500 Hz

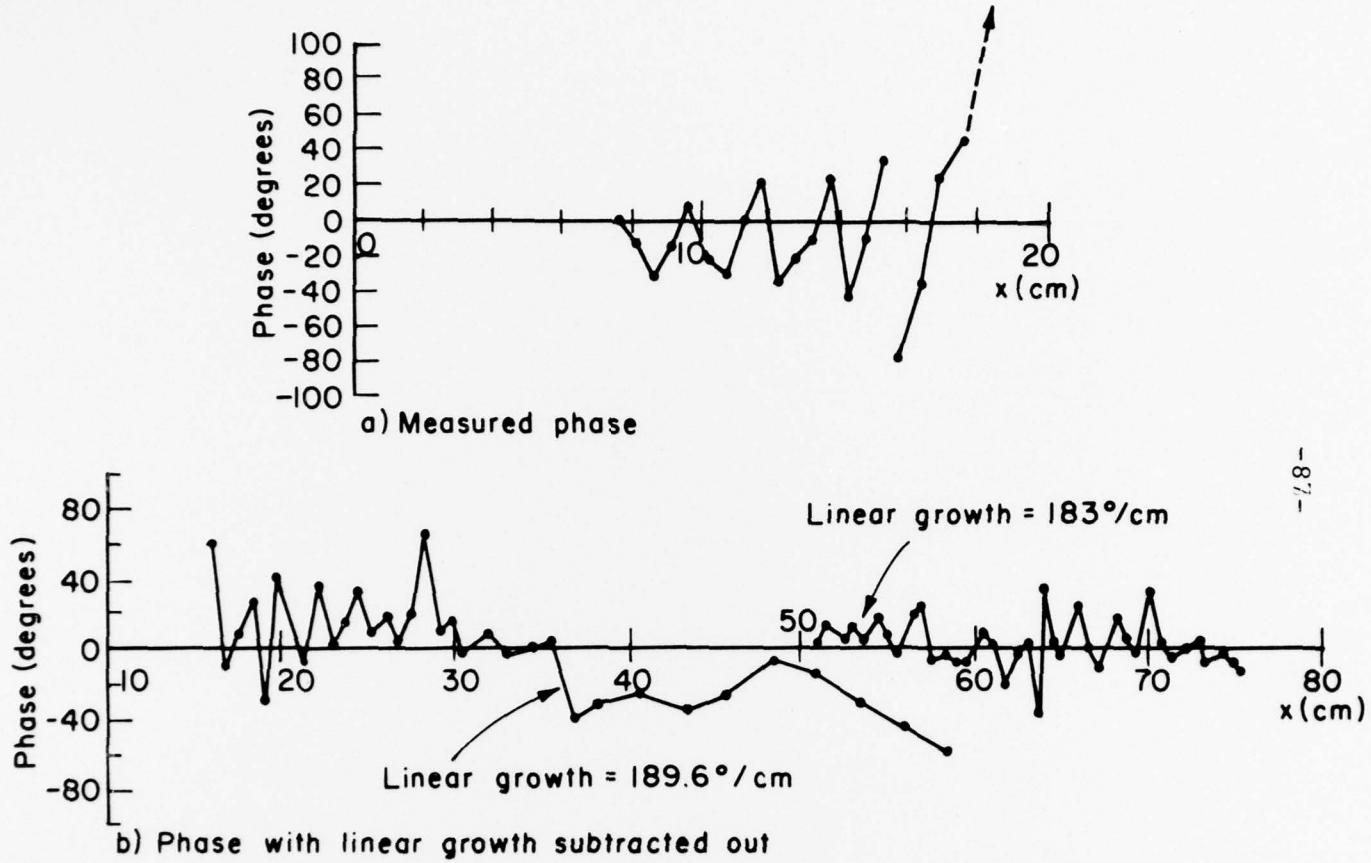

FIGURE 29

PHASE OF EXCITED TOLLMIEN-SCHLICHTING WAVE WITH RESPECT TO PHASE OF THE DRIVING SINE WAVE